# MUSCLE AND TENDON: PROPERTIES, MODELS, SCALING, AND APPLICATION TO BIOMECHANICS AND MOTOR CONTROL

Author: **Felix E. Zajac**
Mechanical Engineering Department
Stanford University
Stanford, California; and
Rehabilitation Research and Development Center
Veterans Administration
Palo Alto, California

Referee: Gerald L. Gottlieb
Department of Physiology
Rush Medical Center
Chicago, Illinois

## I. INTRODUCTION

When the body performs a motor task, the central nervous system (CNS) excites muscles that subsequently develop forces that are transmitted by tendons to the skeleton to effect the task. Thus, muscles and tendons are the interface between the CNS and the articulated body segments. An understanding of the properties of this interface is important to scientists who interpret kinesiological events in the context of coordination of the body, and to engineers who design prosthetic, orthotic, and functional neuromuscular stimulation systems to restore lost or impaired motor function. In all cases, a model of muscle and tendon is used, either explicitly or implicitly.

When movement of the body is analyzed to extract principles of CNS control, often the muscle and tendon model used in the analysis is not explicitly stated. Nevertheless, a model is assumed, even if only implicitly. For example, to assess the contribution of a muscle to movement, conjectures are made based on estimates of muscle force. These estimates, perhaps only qualitative, are at times based on recordings of the electromyographic (EMG) activity in the muscle. Fundamentally, only the level of EMG activity is used to estimate muscle force and then, through comparison with other EMG signals, the role of each muscle in the movement is assessed. In other cases, the force length (fl) and force velocity (fv) properties of muscle, as well as the EMG activity, are qualitatively considered in the estimation of force. Only rarely have the excitation-contraction (EC) properties of muscle or the elastic properties of tendon been included in analyses of force generation.

At other times, models have been explicitly defined, posed mathematically, and used to study coordination and to estimate muscle forces during the motor task, for example, during walking,[1-5] jumping,[6-10] kicking,[11] eye movement,[12-15] and flexion-extension motor tasks.[16-18] The approaches to modeling have ranged from the "reductionist" approach (i.e., models should be based on the microscopic properties of the tissue) to the "black-box" approach (i.e., models only need to be based on an input-output [I/O] description of the tissue). Recent reviews and articles have addressed the utility of each,[19-23] and to some extent this article does also.

Naturally, the model of muscle and tendon to be invoked should depend on the objective. If the fundamental physical and chemical (micro) properties of muscle and tendon are to be understood, then the reductionist approach is clearly justified,[24,25] i.e., to emphasize the study of an elemental unit of muscle or tendon tissue. If the I/O (macro) properties of the

tissue are needed, and if the structure and function of the tissue are completely unknown, then the black-box approach is justified.[26-28] When the structure and function of the tissue are sufficiently specified to define a basis for the macroproperties, then this basis becomes a model for the tissue. The objective then is to identify the parameters of the model. This review synthesizes knowledge of the micro- and macroproperties of muscle and tendon, defines a basis (or model) for the properties of each, and specifies the parameters on which the integrated properties of the musculotendon actuator depend.[22]

Virtually all investigators who study intermuscular coordination use a variation of the classical model of muscle developed in the first half of this century by Hill,[29] Wilkie,[30] and Ritchie and Wilkie.[31] This model has withstood the test of time and is especially noteworthy to studies where the dynamical properties of many muscles must be modeled simultaneously. The model reviewed and developed here is based on a Hill-type model.

Though Hill recognized early that tendon elasticity affects the force generated by muscle,[29,32] the importance of these effects on movement is only now being thoroughly studied.[33-40] This review emphasizes how to assess the role of the tendon in movement through the understanding of how tendon and muscle interact.

Specifically reviewed are

1. The intra- and intercellular organization of muscle and its relation to tendon
2. The EC property of muscle (i.e., *activation dynamics*)
3. The relation among a Hill-type model and the force-length, force-velocity, and stiffness properties of muscle
4. The elastic properties of tendon
5. The properties of muscle and tendon that are generic, and the muscle- and tendon-specific scaling parameters

Specific emphasis is placed on showing:

1. Why muscle and tendon work together as one entity (the *musculotendon actuator*)
2. How the contractility of the muscle and the elasticity of the tendon interact to specify the contraction process of the actuator (the *musculotendon contraction dynamics*)
3. How to synthesize muscle and tendon properties to form a one-parameter model that is generic among all actuators
4. How the one parameter, which is the ratio of tendon length at rest to muscle fiber length at rest, affects the static and dynamic properties of an actuator, specifies the ratio of elastic energy stored in tendon to muscle, and determines whether activation or musculotendon contraction dynamics is rate-limiting
5. How the one parameter affects the frequency response of an actuator, where force is its output, and either actuator length or muscle activation is its input
6. How the frequency response of an actuator can be used to assess whether it behaves as a spring, a dashpot, or a CNS-controlled force generator during a motor task, such as walking
7. How muscle- and tendon-specific parameters scale the properties of the generic actuator
8. Why muscle fiber pennation is expected to only rarely affect the output properties of muscle

## II. PROPERTIES AND MODELS OF MUSCLE

### A. FUNCTIONAL ARRANGEMENT (ARCHITECTURE) OF MUSCLE TISSUE

#### 1. Architecture Among and Within Muscle Fibers

Muscle can be considered to be a collection of equally long fibers (cells) in parallel, where

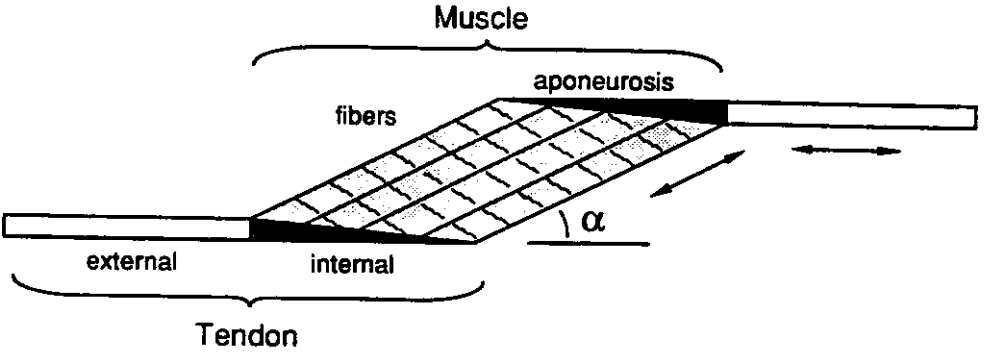


FIGURE 1. Relation among muscle fibers and tendon in a pennated muscle. Muscle fibers (lightly shaded region) lie in parallel, have the same length, and are oriented at some angle α to the tendon axis of pull. Functionally, tendon can be considered to consist of an internal portion (i.e., the aponeurosis of muscle origin and insertion; darkly shaded region) and an external portion. As muscle fibers shorten, muscle is assumed to maintain isovolume, tendon to move only along its axis, and fibers to become more pennated (i.e., α increases). Notice that the fiber and tendon shortening are not colinear (compare the "arrows").

all fibers are oriented either in the direction of the tendon (i.e., a parallel-fibered muscle) or at an acute angle $\alpha > 0$ to the tendon (i.e., a pennated muscle; see Figure 1). Though the relation between muscle fibers and tendon will be described for only pennated muscles, the operational characteristics of a parallel-fibered muscle of volume V can be found from the characteristics of a pennated muscle of volume V, when $\alpha = 0$ is assumed.[41-44] The fibers of a pennated muscle are connected to the aponeurosis of the muscle (i.e., the darkly shaded region in Figure 1), which is also called the "internal" portion of the tendon because its properties appear identical to the properties of the "external" portion of the tendon (i.e., the unfilled region in Figure 1).[37,39,44] The function of the arrangement of fibers shown in Figure 1 seems to capture the essence of the function of even more complex architecture (e.g., bi- and multipennate muscles).[41] Justification for this model has been reviewed elsewhere.[45,46] However, recent data alert us once again to the fact that muscle fibers may not run from internal tendon to internal tendon, as muscle fascicles do, but instead may terminate in the muscle fascicles.[47,48] A muscle fascicle may contain, then, an interdigitated network of fibers, which contain contractile filaments as well as noncontractile, tapered fiber strands. In this review, I assume that muscle fiber length is equal to muscle fascicular length because it is fascicular length that is commonly reported. The assumption can trivially be relaxed, however, if actual muscle fiber lengths are known.

To understand musculotendon mechanics, the effect of pennation on musculotendon function can be ascertained from the arrangement shown in Figure 1 by assuming that muscle is isovolumic and the distance between the aponeurosis of origin and insertion is constant (see Section IV.H).[41-45] Specifically, the major effect is that α, the orientation of muscle fibers to tendon, increases as fibers shorten. Thus, muscle fibers shorten in a direction that is not colinear with the direction in which tendon stretches (Figure 1; compare the arrows). Though this planar representation may also convey the notion that the longitudinal forces in tendon act to rotate muscle fibers, such effects on moving the body segments are believed to be either nonexistent or secondary to the effects caused by the longitudinal forces.[46] Because only very highly pennated muscles affect musculotendon function (see Section IV.H), this review emphasizes other properties of actuators.

A muscle fiber of length $L^M$ can be considered to be a set of homogeneous sarcomeres of equal length $L^S$ that are neurally excited simultaneously to generate the in-series force F (Figure 2). Thick and thin myofilaments (see Figure 2) are the elements of the sarcomere that constitute the basis for the sliding filament and cross-bridge theories of muscle contrac-

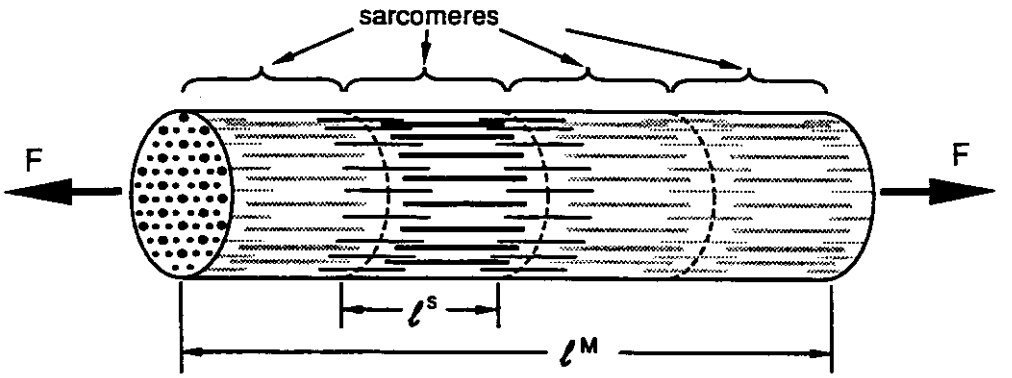


FIGURE 2. Muscle fiber and sarcomere structure. Each fiber (length $L^M$) consists of a series of sarcomeres. Each sarcomere has the same length $L^S$ and experiences the same force F. Myosin myofilaments (dark lines) overlap with actin myofilaments (thin lines), and cross-bridges (not shown) are formed when the sarcomere is activated. Through cross-bridge energetics and the sliding of filaments, the fiber can develop force and shorten.

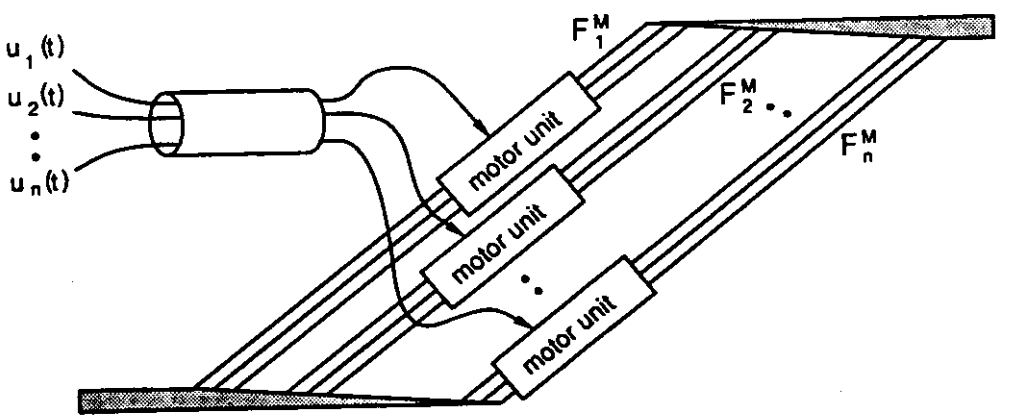


FIGURE 3. Schema of the collective function of motor units of one muscle. Each motor unit is functionally disjoint from the others, including the set of muscle fibers innervated by each motor-nerve axon. The action-potential discharge pattern of each axon *i* ($u_i(t)$ for axon *i*) excites the muscle fibers of that motor unit *i* and generates the collective force $F_i^M$ of the fibers (called the force output from motor unit *i*).

tion.[24,26,49] In this review, the effects of intersarcomere dynamics[50,51] and muscle fiber action-potential propagation on the dynamics of force generation[52] are considered secondary.

## 2. Organization of Muscle Fibers into Functional Units (Motor Units)

A motor unit is defined to be a nerve axon (along with its parent motoneuron in the CNS) and the set of muscle fibers innervated by this axon and its branches.[53] Since a motor unit is thus the smallest functional unit associated with the generation of muscle force, issues related to how the CNS controls net muscle force through the control of individual motor units have been scrutinized (e.g., trade-offs in generating more force by exciting already active motor units more frequently or by recruiting inactive motor units).[53-55] More important to the issues under discussion here are the physiological, histochemical, and biochemical properties of motor units. An almost incontestable conclusion from the many motor unit studies[53,56] is that the innervated muscle fibers of a motor unit have homogeneous properties.

A muscle can thus be represented by *n* motor units being controlled by *n* nerve axons originating from the CNS, each with its own control $u_i(t)$ (see Figure 3). The muscle fibers

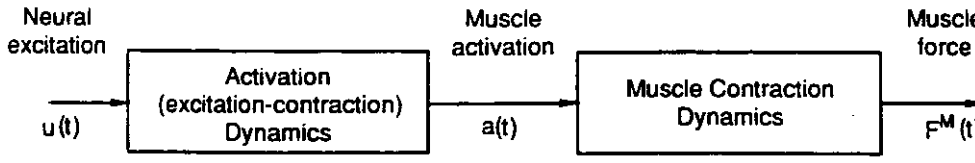


FIGURE 4. Muscle tissue dynamics. CNS excitation of muscle tissue (*neural excitation*, u(t)) acts through *activation dynamics* (EC coupling) to generate an internal muscle tissue state (*muscle activation*, a(t)), which is associated with the $Ca^{++}$ activation of the contractile process. Through *muscle contraction dynamics*, this activation energizes the cross-bridges and *muscle force* $F^M(t)$ is developed.

of each motor unit *i* collectively develop a motor unit force $F_i^M$, which is almost always assumed to sum with the other motor unit forces to produce the net muscle force $F^M$.

Motor units (or muscle fibers, or muscle tissue) are referred to, for example, as "slow contracting" or "fast contracting", and, as implied, the different motor unit types have distinguishable properties.[53,57] Relevant to this review is whether the dimensionless relationships to be developed are generic between slow- and fast-contracting muscle tissue. Indeed, such issues are discussed when appropriate. Many other important issues regarding the different properties of slow- and fast-muscle tissue are ignored in this review (e.g., fatigue and metabolic energetics).[49,53,58,59]

### 3. Muscle Tissue and Scaling

Because of the arrangement of sarcomeres and fibers within a motor unit and their homogeneity in structure, function, and excitation, the properties of a motor unit can be expressed in many ways, all connoting the same information. That is, reference can be made to the functional properties of either a sarcomere, a fiber, or a motor unit. Further, if homogeneity among the motor units of the same type is assumed, then that collection of *muscle tissue* has properties equivalent to any of its fibers, or to any of its sarcomeres, when scaled.[22,41,40,60] Thus the following discussion will at times refer to the properties of *muscle tissue* as though the experiments were performed on a "whole" muscle consisting of many motor units or muscle fibers (and sometimes they are).

Emphasis is placed on the generic relations that specify muscle tissue function, and how muscle size scales these relations. For example, the fl and fv properties of a muscle are assumed to be just scaled-up versions of the properties of muscle fibers, which are in turn assumed to be scaled-up versions of properties of sarcomeres.

## B. CONTRACTION DYNAMICS OF MUSCLE TISSUE

The dynamics of muscle tissue can be divided into activation dynamics and contraction dynamics. *Activation dynamics* corresponds to the transformation of neural (or artificial) excitation to activation of the contractile apparatus, and *muscle contraction dynamics* to the transformation of activation to muscle force (see Figure 4). Contraction dynamics is discussed in this section.

### 1. Force-Length Property

The steady-state (static) property of muscle tissue is defined by its isometric fl curve, and this property can be studied when activation a(t) and fiber length $L^M$ are constant. Full activation (i.e., a(t) = 1) will occur when muscle tissue has been maximally excited (i.e., u(t) = 1) for a long time. The reason muscle must be excited for a long time for a(t) = 1 is that activation transients must subside and steady-state must ensue (see Figure 4, *activation dynamics*). Conversely, muscle tissue that has been neither neurally- nor electrically-excited for a long time is said to be inactivated, or passive (i.e., u(t) = a(t) = 0).

Both passive and fully activated muscle tissue develop a steady force when held isometric

(see Figure 5A).[49,57,61,62] The difference in force developed when muscle is activated and when muscle is passive is called *active muscle force* (Figure 5A, *active*). The region where active muscle force is generated is (nominally) $0.5L_o^M < L^M < 1.5L_o^M$, where $L_o^M$ is the length at which active muscle force peaks (i.e., $F^M = F_o^M$, when $L^M = L_o^M$; $L_o^M$ is called muscle fiber resting length or *optimal muscle fiber length*).[41-43,57,62,63] Notice that the shortest length at which passive muscle tissue develops force is (nominally) $L_o^M$.[57] Though the passive tension of muscle (i.e., a collection of fibers) has been thought to be due to interfiber connective tissue (e.g., endomysium, perimysium, and epimysium),[49,61,64,65] recent data suggest that the resting tension of muscle arises instead from intrafiber (myofibrillar) elasticity.[66] The reason previous data may have led to the conclusion that passive tension is due to interfiber elasticity is that this data had been collected from musculotendon tissue, not from muscle tissue in isolation. That is, since not all of the tendon had been removed from these preparations, the methodology used to infer that passive tension in muscle fibers develops at lengths less than $L_o^M$, which is the basis for the conclusion, may have been flawed (see Section IV.C).

The fl property of less than fully activated muscle tissue can be considered to be a scaled version of the fully activated one (compare Figure 5B with Figure 5A).[16,22] Less than full activation of muscle tissue can occur when some or all of the fibers are less than fully excited. One way this can occur naturally is when some motor units are inactive. Another way is when activated motor units are neurally excited by low-frequency pulse trains; the activation of these units will then, on average, be less than one (e.g., a motor unit is less than fully activated during a twitch).[57] The scaling of the fl curve by activation is consistent with the almost universal assumption that forces generated by muscle fibers (units) in parallel sum (e.g., see Figure 3; however, see Partridge and Benton[23]) and that forces generated within a fiber also sum (i.e., cross-bridges are independent and their forces sum).[25,49] However, some studies suggest that the zero-force intercept at low muscle fiber lengths depends on activation.[67,68] The passive fl curve has always been assumed to be unaffected by a(t) (see Figures 5A and B).

## 2. Force Velocity Property

When fully activated muscle tissue is subjected to a constant pull (tension), it first shortens and then stops (i.e., muscle tissue undergoes an *isotonic contraction*). The length at which shortening terminates corresponds to the length at which such a force can be sustained in steady-state (i.e., as specified by the isometric fl relation when $a(t) = 1$).[69,70] From a set of length trajectories, obtained by subjecting muscle to different tensions, an empirical fv relation can be constructed for any length $L^M$, where $0.5L_o^M < L^M < 1.5L_o^M$ (e.g., see Figure 5C).[23,70] The fact that the observed length trajectories can be described well by integrating the inverted velocity-force expressions[70,71] supports the use of a force-length-velocity-relation (an *flv relation*) to model muscle behavior. Finally, at optimal fiber length $L_o^M$, a *maximum shortening velocity* ($v_m$) can be defined from the fv relation (see Figure 5C).[29] At this velocity $v_m$, muscle cannot sustain any tension, even when fully activated.

When *empirical* fv relations are constructed for lengths $L^M < L_o^M$, the velocity at which no tension can be sustained (i.e., the velocity-axis intercept) is found by extrapolation to be less than $v_m$.[69-72] However, the sliding-filament *theory* for muscle contraction (i.e., our understanding of muscle function at the micro level) predicts that the velocity-axis intercept should be independent of sarcomere length, at least for lengths $L^M \geq L_o^M$.[24,25,49] The theory also predicts that $v_m$, at the single-fiber level, should be independent of activation, which can be controlled *in vitro* by changing the Ca ion concentration. Some experiments on single fibers suggest, however, that the velocity-axis intercept is length or activation dependent, especially when $L^M$ and a(t) deviate greatly from $L_o^M$ and 1, respectively (e.g., see Figure 5D).[73-77] The issue of the invariance of the velocity-axis intercept to $L^M$ and a(t) is not only unresolved, but hard to resolve because a perfect no-load condition (i.e., $F^M = 0$) is difficult to achieve, and the sensitivity of velocity to force is high near $F^M = 0$.

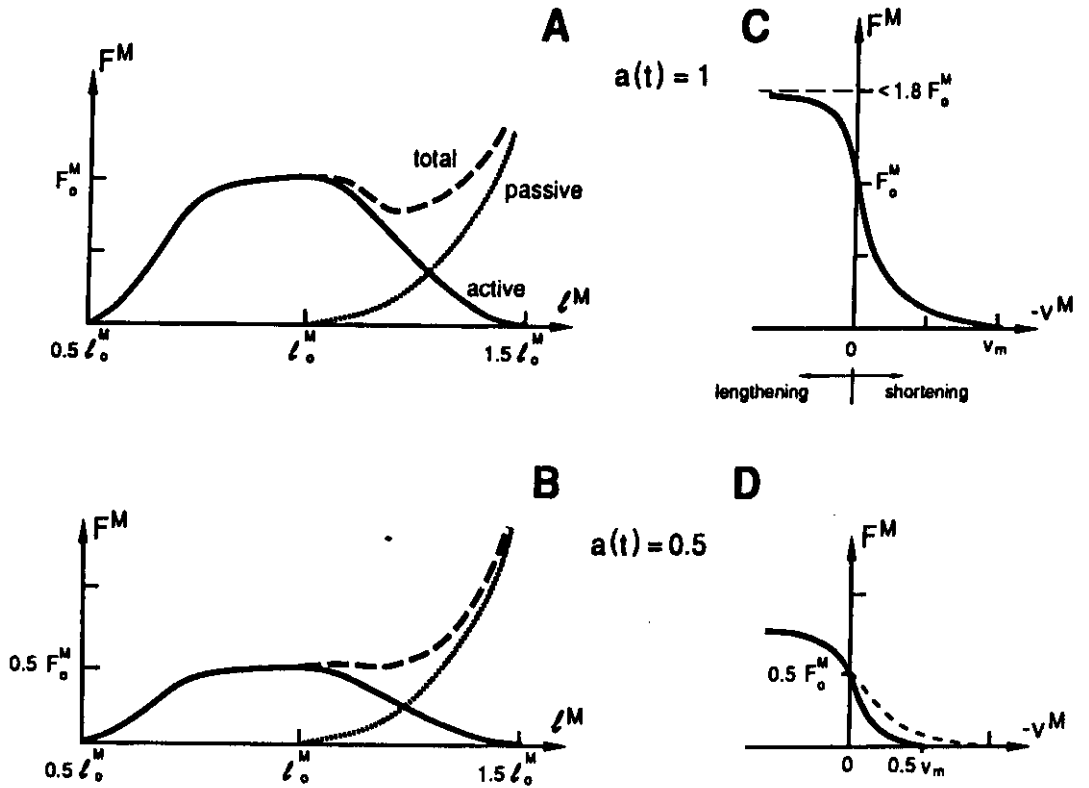


FIGURE 5. Nominal static and dynamic properties of muscle tissue. (A) Isometric force length (fl) relation of muscle tissue when *passive* (dotted curve) and when fully activated (dashed curve). Net force contributed by the activation of muscle tissue is the difference, called *active* force (solid line). By definition, peak active force $F_o^M$ is developed when fibers are at their optimal length (i.e., when $L^M = L_o^M$). (B) Less than fully activated muscle tissue develops proportionately less active force (solid line), but passive force is unchanged (dotted line). (C) Force velocity (fv) relation of fully activated muscle tissue when fibers are at a length $L^M = L_o^M$. An applied constant force less (greater) than $F_o^M$ causes muscle tissue to shorten (lengthen). Limits exist to force generation ($<1.8F_o^M$) and to muscle fiber shortening ($v_m$). $v_m$ is called the *maximum shortening velocity*. (D) Less than fully activated muscle tissue has been assumed either to shorten at a rate less than $v_m$ when unloaded (e.g., refer to intercept of

However, the issue of the invariance of the velocity-axis intercept to $L^M$ and a(t) may be a moot one to muscle-coordination studies. To date, it does not seem to make any difference which assumption is invoked. Many investigators who model muscle to study muscle coordination choose to assume that the velocity-axis intercept is constant;[21,22,78] others assume that the intercept decreases with length and activation.[12,16,79] One reason for the indifference is that muscle neither produces any power output at zero force nor exists in a state near zero force for very long (otherwise full joint excursion would be very quickly reached). Thus, energy output when muscle operates near the zero-force state is low. Thus, though a topic of concern to micro-level theories of muscle contraction, this issue may just be functionally unimportant at the muscle-coordination level.

The shape of the fv curve determines the mechanical power output ($F^M \cdot -v^M$) that active muscle delivers. During shortening, muscle delivers power (power output is positive), with peak power output occurring when muscle shortens at $\sim 0.3 v_m$.[29,49] When a motor task requires net propulsion, clearly some muscles must shorten some of the time during the task. However, many tasks require the net absorption of potential and kinetic energy of the body segments (e.g., during descending stairs and decelerating to a complete stop). The only way body-segmental energy can be dissipated is by energy absorption by muscle, assuming that frictional losses at the joints, in tendons, and elsewhere in the body, as well as at the contact surfaces between the body and external objects (e.g., the stairs), are negligible. Thus muscle must lengthen while under tension to absorb power. But if muscle fibers lengthen too fast, they can be injured.[80]

Thus, the shape of the fv curve during lengthening is also important to computer simulation of movement. Unfortunately, there are only a few studies where higher-than-peak isometric force has been applied to muscle tissue. Isotonic experiments show that the greater the applied tension is, the faster the muscle lengthens (see Figure 5C), though the ultimate tension a muscle can sustain is limited to 1.1 to $1.8F_o^M$.[81-83]

To summarize, virtually all computer models of muscle used in studies of muscle coordination employ the same-shaped fv curve (e.g., see Figure 5C). Common assumptions are that (1) the fv relation scales with length and activation in one of two ways (i.e, either the velocity-axis intercept remains constant under all conditions or decreases with a(t) and $L^M$ [e.g., see Figure 5D]); (2) no discontinuity in slope at $F_o^M$ exists, even though experiments and cross-bridge theory suggest one;[24,29,81] and (3) the fv curve at any instant is unaffected by preceding events, even though it is known that prestretched muscle tissue subsequently shortens faster.[84-86] At the moment, therefore, it seems that other issues influence our understanding of muscle coordination more than our knowledge of the exact shape of either the shortening or lengthening regions of the fv curve.

## 3. Mechanical (Hill-Type) Model of Contraction Dynamics

A conceptual, Hill-type model is that the contractile properties of muscle tissue can be represented by a flv relation controlled by muscle activation (see Figure 6). Basically, both a *passive element* (PE) and an in-parallel *contractile element* (CE) are assumed to contribute to muscle force $F^M$. Importantly, the force $F^{CE}$ is assumed to depend only on the current length $L^M$, velocity $v^M$, and activation a(t), and is assumed to be specified by some expression compatible with the notions discussed above (e.g., see Figure 5). Commonly, Hill's equation[29] is modified and used as the expression,[19,21] though nothing precludes the use of other expressions.[22] Sometimes a muscle elastic element, distinguishable from tendon elasticity, is included in series with the CE (dotted line in Figure 6).[3]

The motivation to separate muscle elasticity from tendon elasticity is that estimates of energy stored in muscle cross-bridges compared with energy stored in tendon is desired in studies of the biomechanics of movement.[34,37] Energy is putatively stored in cross-bridges because active muscle tissue exhibits stiffness that presumably arises from the cross-

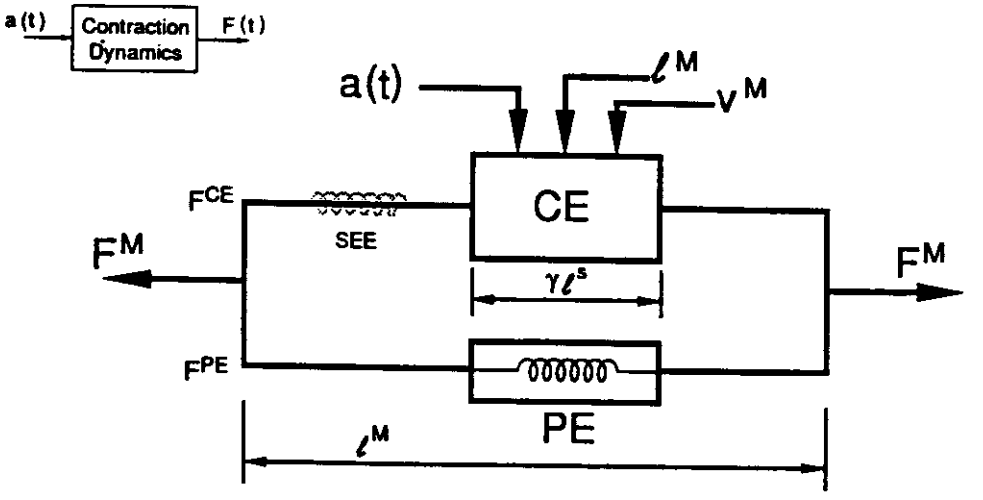


FIGURE 6. Hill-type model for contraction dynamics of muscle tissue (inset). Total muscle force $F^M$ is the sum of passive force $F^{PE}$ and active force $F^{CE}$. Structures putatively responsible for these forces are called the *passive element* (PE) and the *contractile element* (CE). Force $F^{CE}$ depends on muscle fiber length $L^M$ and velocity $v^M$, and the state of activation of the muscle fibers a(t). Some models include a *muscle series elastic element* (SEE). The length of the CE is the sum of the lengths of the $\gamma$ sarcomeres of a muscle fiber (i.e., $\gamma L^S$) and differs from muscle fiber length $L^M$ by the length of the SEE.

bridges.[25,87-89] However, in all but short-tendon actuators, the energy stored in cross-bridges is expected to be very small compared with the summed energy stored in the external and internal parts of tendon (see Section IV.I and Alexander and Bennet-Clark,[34] Rack et al.,[38] and Rack and Westbury[39]). Thus, for many actuators, tendon compliance dominates and muscle series elastic element (SEE) can be neglected (see solid line in Figure 6).

Another reason for disregarding muscle SEE, as shown in Figure 6, is that situations antithetical to the basic notion of sarcomeres and fibers acting in concert would otherwise arise. For example, with a muscle SEE, muscle fiber length would not be proportional to sarcomere length, and the static properties of fibers would not be scaled versions of the static properties of sarcomeres. Notice from Figure 6 that sarcomere length $L^S$, multiplied by the number of sarcomeres $\gamma$, corresponds to the length of the CE ($\gamma L^S$), and fiber length corresponds to $L^M$. Thus, the length of a muscle fiber and its sarcomeres are not proportional because of the stretch in the muscle SEE. Consequently, the fl relation of a fiber is no longer a length-scaled version of the fl relation of a sarcomere. The muscle fiber fl relation will instead be a distortion of the sarcomere fl relation.[31]

Furthermore, with a muscle SEE, muscle fiber velocity will not be a scaled version of sarcomere velocity. For example, consider the case when muscle fibers are isometric and initially at rest. Muscle force will then gradually rise to its isometric value on full activation because sarcomere length, as evident by CE length ($\gamma L^S$), becomes shorter as the muscle SEE stretches (see Figure 6). Thus, muscle fibers will be isometric (i.e., muscle fiber length will be constant), yet sarcomeres will shorten (i.e., the CE will shorten).

With a muscle SEE, muscle fiber velocity could even be directionally *opposite* to sarcomere velocity should muscle force change rapidly (say, decrease fast) and muscle fiber velocity change slowly (in this case, shorten slowly). Hypothetically, then, because of the rapid decrease in force, the muscle SEE would shorten faster than the slowly shortening muscle fibers, causing the sarcomeres (i.e., the CE) to lengthen. To have sarcomere and muscle fiber velocity directionally opposite is incompatible with our notion of sarcomere-to-fiber scaling and with the sliding-filament theory.[24,25,49] In my opinion, the obstruction of the association of the elements in Figure 6 with anatomically defined components (e.g., sar-

comere length and velocity with muscle fiber length and velocity, respectively) is a major deterrent to the inclusion of a muscle SEE in a muscle model.

Muscle SEE, when associated with cross-bridge stiffness, can thus be neglected completely, with little inaccuracy, except when coordination studies involve short-tendon actuators (see Equation 31 for how much inaccuracy occurs, and Section IV.B for how to define "short-tendon actuators"). However, for completeness, cross-bridge compliance could be summed with tendon compliance into one element in series with, but external to, the structures shown in the boxes in Figure 6.[10,12,22,70,79] If muscle and tendon were to constitute a linear system, the I/O properties of such an actuator could be made indistinguishable from the I/O properties of one having its muscle SEE as shown by the dotted line in Figure 6.[40,90]

Regardless, muscle stiffness will have to be modeled when short-tendon actuators are subjected to quick stretches. The reason is that force transients will very much depend on muscle stiffness. However, the modeling of stiffness per se,[91] or movements in which quick transients play an important part (e.g., the coordination of muscles at heel-strike during running), will probably demand more complex models than a Hill-type model (see Section V).

Finally, should thin myofilaments or Z-lines be shown to be extensible,[92] contrary to current belief,[87,88] the inclusion of a muscle SEE, as shown in Figure 6, would be justified. In this case, the length of the CE would be associated with the length of the thick filaments, and the length of the SEE would be associated with the summed length of the thin filaments and Z-lines.

## C. ACTIVATION DYNAMICS OF MUSCLE TISSUE

### 1. Excitation-Contraction Coupling (EC)

The information content of the neural excitation to a motor unit is contained in the sequence of motor unit discharges. Since the innervated muscle fibers discharge in virtual synchrony with one another and with the discharges of the distal (muscle) end of the nerve fiber and its branches, this excitation of neural and muscular tissue can be referred to as "neuromuscular excitation", or simply *neural excitation* (see Figure 4). Similarly, the neural excitation of any set of simultaneously activated muscle fibers, where a lumped parameter model is used to model the collective dynamics of the fibers, is specified by the discharge sequence of the fibers.

Neural excitation (see Figure 4, u(t)) is coupled to the contractile machinery through an intermediate variable, which is called *muscle activation* (see Figure 4, a(t)), or just *activation*, but otherwise is identical to Hill's original notion of an "active state".[29,32] EC coupling is mediated by calcium dynamics.[25,93,94] The kinetics associated with the intracellular processes of calcium activation and deactivation of the contractile machinery are often approximated by first-order dynamics to simulate the dominant (slowest) first-order chemical-kinetic reactions of EC coupling.[95-97] Important characteristics of activation (EC) dynamics are that the rate constant for activation is greater than for deactivation, and activation has saturation.

Virtually all models used to study body-segmental coordination assume that activation dynamics is uncoupled from the subsequent force-generating process (i.e., muscle contraction dynamics). However, some studies *in vitro* suggest that EC coupling and cross-bridge mechanics are coupled, though the issue is far from resolved and the conditions defining such coupling are unclear.[68,93,98] For simplicity, I assume, as others have, that activation and muscle contraction dynamics are uncoupled (see Figure 4).

### 2. Association of Activation with Isometric Force

The recording of isometric active-muscle force is a way of measuring muscle activation to a specific neural excitation. In a model devoid of a muscle SEE, the muscle time-varying active force $F^{CE}(t)$ is a function of only a(t), $L^{M}(t)$, and $v^{M}(t)$ (see Figure 6). In an isometric

contraction, $L^M$ = constant and $v^M = 0$. $F^{CE}(t)$ is thus given only by the time-varying input a(t). Since a(t) is assumed to scale the isometric, active muscle fl curve (see Figures 5A and 5B, solid lines), and $L^M$ is constant, the muscle active force $F^{CE}(t)$ is proportional to activation a(t) in an isometric contraction.

However, if a model should include a muscle SEE, $F^{CE}(t)$ would lag a(t), though it can be shown that if the properties of the muscle SEE should be chosen to correspond to the stiffness of the cross-bridges, this lag would be small relative to the lag caused by activation dynamics (unpublished results). Stated differently, I believe activation dynamics is the rate-limiting step in force development in preparations devoid of tendon and muscle aponeurosis elasticity (e.g., in isolated muscle fiber preparations); however, when such elasticity does exist, as *in situ*, activation dynamics may no longer be rate-limiting (see Section IV.G).

Given the correspondence between isometric force and activation, it follows that muscle activation is a complex function of the sequence of neural pulses. The reason is that the twitch depends in a complex way on the past history of excitation (e.g., as evident by post-tetanic potentiation and depression, and the manner in which force develops to a train of pulses).[57,99-101] However, nonlinear models of EC coupling based on calcium dynamics can model many of these properties.[95,102]

Finally, though activation of muscle can be associated with isometric muscle force, isometric experiments on muscles are often, in reality, isometric experiments on the musculotendon actuator (i.e., the length of muscle *plus* tendon is held constant, rather than the length of muscle alone). In this case, the force recorded does not represent the activation of the muscle, but, because of muscle fiber shortening, instead represents a low-pass filtering of the activation (see Section IV).

## D. SINGLE-INPUT, SINGLE-OUTPUT (SISO) MODEL OF MUSCLE

Ideally, a model of muscle should account for the individual characteristics of motor units. After all, it is the discharges of single motoneurons that excite individual motor units that collectively generate the muscle force (see Figure 3). No such complex representation of muscle has been used in models designed to study coordination, nor is such complexity justified at the moment (see below). In fact, very little experimental work has been done to test the concept that the forces developed from individual motor units should sum to produce muscle force (see Figure 3).[103] Similarly, very few models have been developed to study the integrated muscle force-generating capability of motor units that are simultaneously controlled (excited) by desynchronized neural pulse trains. It is even unusual to find models that predict the collective force-output from muscle that is composed of different type motor units, all of which are maximally excited (i.e., a(t) = 1). For example, the concepts noted above and expressed in Figures 3, 5, and 6 suggest, trivially, that the net isometric muscle force curve should be the sum of the individual motor unit fl curves. Unexpectedly, perhaps, is the prediction that the net fv curve for muscle should have more curvature than the fv curve of any one unit, if muscle tissue should be divided into motor units having different maximum shortening velocities (unpublished analysis). Though this prediction may not be well recognized, it has usefulness to the lumped-parameter modeling of muscle, which is discussed next.

### 1. Rationale for a SISO Muscle Model

Most muscle models used in computer studies of coordination have one input, which represents the collective excitation of muscle, and one output (muscle force or, equivalently, tendon force). Many of these models assume that the overall system can be adequately represented by second-order dynamics, i.e., a first-order dynamical process, associated with activation dynamics, cascaded and decoupled from another first-order dynamical process, associated with contraction dynamics. Thus, the net neural excitation u(t) acts through the first-order

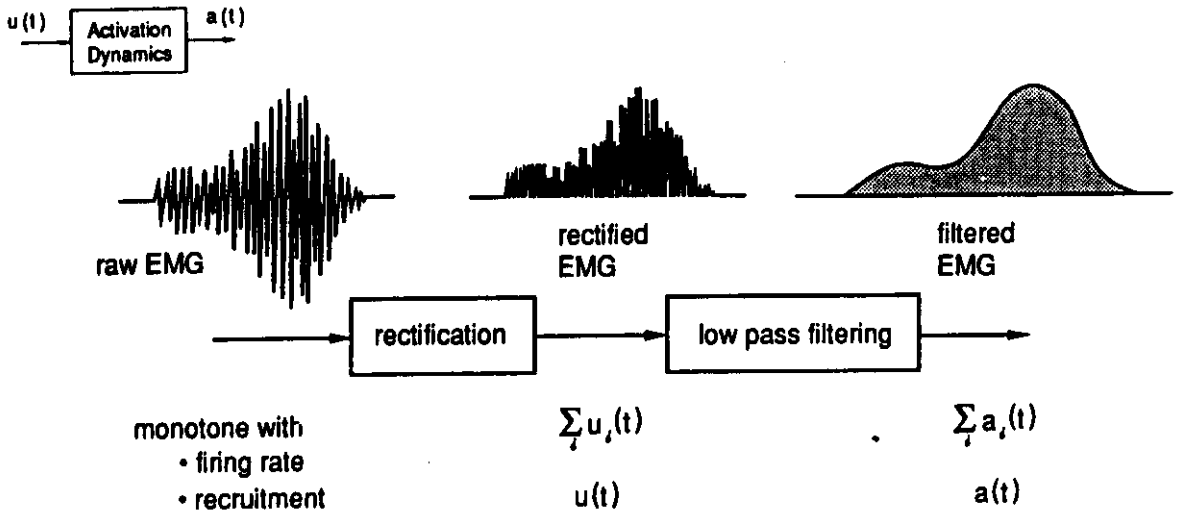


FIGURE 7. Association of activation dynamics (inset) with EMG activity in a SISO muscle model. *Raw EMG* activity increases both as the firing rate of individual motor units rises and as previously inactive units become recruited. The envelope of the raw EMG (*rectified EMG*) can be considered to be the net neural drive to the muscle u(t), which is related (somehow, e.g., by $\Sigma u_i(t)$) to the combined motor-unit drive. The filtered, rectified EMG (*filtered EMG*) can be related to the net activation of the muscle a(t) (somehow, e.g., by $\Sigma a_i(t)$), especially when the EMG, low-pass filter characteristics are set to correspond to those of activation dynamics.

activation dynamics to produce a net activation a(t) (see Figures 4 and 7), which sets a specific flv relation for muscle (see Figures 5 and 6). This flv relation, together with tendon elasticity, establishes a first-order musculotendon dynamical process (see Section IV). Since a muscle SEE is excluded in the specific formulation to be used in this review, tendon must be included for contraction dynamics to be first-order (thus the name *musculotendon contraction dynamics*). If muscle should be assumed to have a SEE, a first-order contraction-dynamics process would be associated with muscle, even in the absence of tendon. If both a muscle SEE and a tendon should be included in a model, contraction dynamics would again be first-order and the term *musculotendon contraction dynamics* would still be meaningful.

The major reasons for using a SISO model are

1. The dynamics to describe a motor task quickly becomes high dimensional. For a second-order model of muscle, the number of state variables is (2m + 2n), where m = number of muscles and n = number of degrees-of-freedom of the mechanical system being used to model coordination. The interpretation of data from computer simulations having this number of state variables is challenging enough intellectually, and the computational time required to solve such models is long when (m + n) is large.
2. The state variables associated with forces developed by muscles (i.e., $F^M$ or, equivalently, tendon force) can be compared to forces computed from experimental data. For example, the net moment about a joint produced from the forces of actuators crossing that joint can be estimated from inverse dynamical analysis of experimental biomechanical data.[104] This net muscle moment can be compared to the net moment derived from a computer simulation of the task, which must contain both a model for the force developed by each of the actuators as well as a model of each of their moment arms (i.e., a model of the musculoskeletal geometry).[105]
3. The state variable associated with muscle activation a(t) and the neural-excitation input signal u(t) can also be related to experimental data. For example, experimental records of EMG can be processed for comparison with muscle input and activation signals (see Figure 7). The envelopes of the rectified EMG and of the filtered, rectified EMG can be compared with u(t) and a(t), respectively.[17,19,79,106] Simple first-order dynamics can be used to represent this EMG-to-activation process, including a bilinear differential equation[106a]

$$\frac{d\,a(t)}{d\,t} + \left[\frac{1}{\tau_{act}} \cdot (\beta + [1-\beta]u(t))\right] \cdot a(t) = \left(\frac{1}{\tau_{act}}\right) \cdot u(t)$$

$$0 < \beta = \text{const.} < 1 \qquad (1)$$

Notice that the *rate constant* $(\frac{1}{\tau} \cdot [\beta + (1-\beta)u(t)])$ associated with this first-order dynamics is linear in the amount of excitation u(t), and increases when u(t) > 0, since $0 < \beta < 1$. Therefore, in fully excited muscle (u(t) = 1), activation dynamics is assumed to be at its fastest, having its highest rate constant of $1/\tau_{act}$, and at its slowest when u(t) = 0, when its rate constant is only $\beta/\tau_{act}$. Therefore, $\beta$ is the parameter that specifies the ratio of these two rate constants. Or, equivalently, this model assumes that the *time constant* for buildup in activation of a fully excited muscle (i.e., $\tau_{act}$) is less than the time-constant for full relaxation of activation (i.e., $\tau_{act}/\beta$, defined as $\tau_{deact}$), and $\beta$ is the parameter setting the ratio of these two time-constants (i.e., $\beta = \tau_{act}/\tau_{deact}$). Thus, the time constants for buildup and relaxation of activation can be defined:

$$\tau_{act} = \textit{time-constant} \text{ when muscle is fully excited } (u(t) = 1)$$

$$\tau_{deact} = \tau_{act}/\beta = \textit{time-constant} \text{ when muscle is deactivated } (u(t) = 0)\ (0 < \beta < 1) \qquad (2)$$

Since activation and isometric tension are proportional (see above), one consequence of this model is that active isometric force rises faster during excitation than it falls during relaxation, a property of muscle that is well documented.[12,16,17,30-32,49,57,70,79,95-97,102]

4. Even if the computational challenge is overcome, and modeling the constituent motor units of muscle becomes intellectually desirable, techniques are unavailable to consistently record unitary activity from many single-motor units during movement. Thus, though unitary activity via computer models can be generated, comparisons with experimental data are impossible. Even the intermediate modeling step of grouping motor units into, say, two sets, a slow-contracting set and a fast-contracting set, does not seem worthwhile, since the same experimental limitation applies.

Some models have dissociated the firing-rate control of a muscle from recruitment control.[22,107] In a SISO model, these two controls are indistinguishable. Nevertheless, since the EMG is monotone with each control (see Figure 7), the SISO model is at least consistent with each (i.e., when u(t) increases in the model, the implication is that either already active motor units discharge faster, or more motor units are recruited, or both). And given that both the discharge rate and the recruitment of motor units increase with excitatory drive to the motoneuronal pool,[55,108] a single control u(t) (i.e., the EMG) can meaningfully be construed as the *net* neural control signal to the muscle. Finally, if separate controls for firing rate and recruitment should be invoked in models, there would again be conceptual limitations; there is neither a way to process the EMG nor a way to process unitary activity to arrive at either a net firing rate or a net recruitment level without making many assumptions as to the underlying unitary events. Thus, I believe the added complexity cannot be justified at this time.

The comments above presume that the muscle model will be used to study human coordination. However, techniques have been developed to record unitary events in animals during movement,[109] and there may well be a greater need for more complex models than implied above. If the need for more complex muscle models should arise, the favorable implication would be that coordination of animal movement would be better comprehended than it is now.

## 2. Muscle Material Properties and Scaling

In modeling many muscles to study coordination, as in the modeling of any large-scale system, trade-offs between simplicity and complexity in the model structure and between few and many parameters must be made. To comprehend how muscles affect coordination of body segments, a sizable number of body segments and muscles must be studied. For practicality and so that interactions among the body segments and muscles can be emphasized in a study rather than the secondary and tertiary properties of any one muscle, it is desirable to develop a generic muscle model that can be scaled by few parameters to represent a specific muscle.

From the above discussion, it seems reasonable to formulate a generic SISO model based on the following material properties of muscle:

1. A dimensionless force-length curve of passive muscle (see Figure 8A)
2. A dimensionless force-length curve of active muscle (see Figure 8A)
3. A dimensionless force-velocity curve (see Figure 8B)
4. A dimensionless first-order activation-dynamics equation (e.g., derived from Equation 1; see below)

With this formulation, the muscle-specific parameters needed to scale the above material properties to generate the structural and the dynamic properties of a muscle are

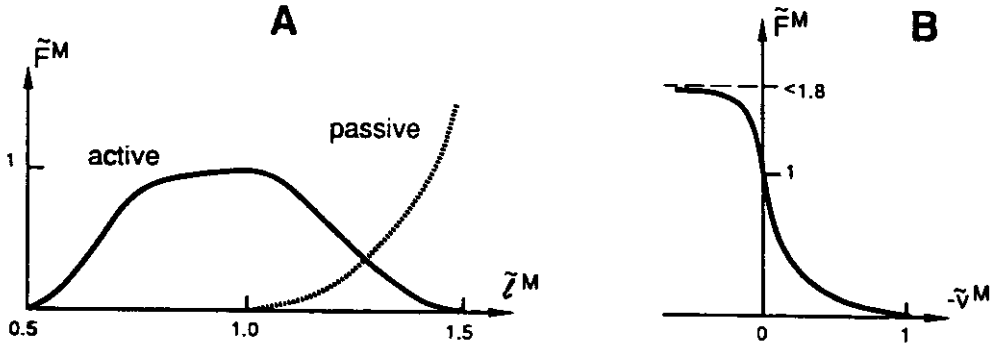


FIGURE 8. Material properties of muscle tissue. (A) The generic, static properties of *passive* muscle (the PE) and *active* muscle (the CE) are given by their dimensionless fl curves. $\tilde{F}^M$ and $\tilde{L}^M$ are force $F^M$ and fiber length $L^M$ normalized by peak force $F_o^M$ and optimal fiber length $L_o^M$, respectively. (B) The generic, dynamic property of muscle (the CE) is given by its dimensionless fv relation. Note that $\tilde{v}^M$ is $v^M$ normalized by the maximum shortening velocity $v_m$ of the muscle (i.e., $\tilde{v}^M \equiv v^M/v_m = v^M/(L_o^M/\tau_c)$ since $v_m = L_o^M/\tau_c$; $\tau_c$ is called the *time-scaling parameter*).

1. Peak isometric active force ($F_o^M$)
2. Optimal muscle fiber length ($L_o^M$)
3. Optimal muscle fiber pennation angle ($\alpha_o$) where $\alpha_o$ is the fiber pennation when $L^M = L_o^M$
4. Maximum shortening velocity $v_m$, normalized by $L_o^M \left(\frac{1}{\tau_c}\right)$ where

$$\frac{1}{\tau_c} \equiv \frac{v_m}{L_o^M}$$

is called the *normalized maximum shortening velocity* and

$$\tau_c = L_o^M / v_m \tag{3}$$

is called the *time-scaling parameter*, in units of seconds.

Implicit to this formulation is that $F_o^M$ and $L_o^M$ scale all force and length quantities, respectively (e.g., the passive and active fl curves). Basically, all models and experimental paradigms invoke this assumption. Thus, the force- and length-related material properties of muscle are believed to be identical among slow and fast muscle tissue;[57,110] however, force per unit area may depend on tissue type (see below).

Also implicit to the formulation is that $\tau_c$ scales time, i.e., a dimensionless time can be defined from Equation 3:

$$\tau \equiv \left(\frac{1}{\tau_c}\right) \cdot t \tag{4}$$

Thus, the velocity axis of the fv curve is assumed to be scaled by the maximum shortening velocity of muscle (i.e., by $L_o^M/\tau_c = v_m$, see Equation 3), and the force axis by $F_o^M$, which are assumptions that are almost always invoked because of the plethora of supporting experimental data.[25,49,57] Even though it is well known that fast and slow muscle tissue have differently shaped fv curves (i.e., fast muscle tissue has less curvature),[57,111-114] the formulation above assumes identically shaped fv curves for all muscle tissue types (see Figure 8A). Given that the focus is on the development of a SISO model, that most muscles are mixed,[115,116] and that model simplicity is desired, I believe this assumption fosters the

acquisition of insight into the dynamical properties of muscles and musculotendon actuators. The assumption can always be relaxed.[16]

In the above formulation, all muscles are assumed to have the same activation dynamics. Therefore, all muscles are assumed to have the same constitutive, dimensionless first-order activation dynamics equation. One possible equation can be derived by first defining dimensionless activation and deactivation time constants, analogous to those in Equation 2.

$$\tilde{\tau}_{act} \equiv \tau_{act}/\tau_c = \textit{dimensionless activation time constant}$$

$$\tilde{\tau}_{deact} \equiv \tau_{deact}/\tau_c = \tilde{\tau}_{act}/\beta = \textit{dimensionless deactivation time constant} \tag{5}$$

and then substituting Equations 5 and 4 into Equation 1:

$$\frac{da(\tau)}{d\tau} + \left[\frac{1}{\tilde{\tau}_{act}} \cdot (\beta + [1 - \beta]\, u(\tau))\right] \cdot a(\tau) = \left(\frac{1}{\tilde{\tau}_{act}}\right) \cdot u(\tau)$$
$$0 < \beta = \text{const.} < 1 \tag{6}$$

Notice from Equations 2 and 5 that $\beta$ is the ratio of the activation time constant to the deactivation time constant, regardless of whether the time constants are expressed in units of time or are dimensionless (i.e., $\beta = \tilde{\tau}_{act}/\tilde{\tau}_{deact} = \tau_{act}/\tau_{deact}$).

So, the question becomes, Is it reasonable to assume that activation dynamics is muscle-independent except for time scaling? I believe the answer is yes. But before presenting the rationale, recognize that a direct consequence of this assumption is that isometric muscle-force trajectories are being assumed to be muscle-tissue-type independent, except for scaling in force and time. The rationale is based on the fact that activation dynamics of slow and fast muscle tissue differ in time scaling by about the same amount as their $\tau_c$ values. That is, it is known that the normalized maximum shortening velocities (i.e., $v_m/L_o^M$) of slow and fast muscle tissue differ by about 2 to 3 times.[57,111,113,114,117,118] The activation dynamics of these tissues also differ by about 2 to 3 times, as is evident by both the twitch contraction time and the time constant for isometric force development during maximal excitation.[53,56,57,114,118-120] Therefore, an approximation to modeling activation dynamics of slow muscle tissue is to model it exactly as one does fast muscle, except for a scaling in time. The scaling factor is given by the ratio of their normalized maximum shortening velocities or, equivalently, by the ratio of their $\tau_c$ values.

Can the number of muscle-specific parameters be reduced further? $F_o^M$ and $L_o^M$ are not candidates, since they differ greatly, at least among limb muscles in animals and humans.[44,121-125] It should be noted that the physiological cross-sectional area ($A^M$) of muscle (i.e., total area normal to the longitudinal axis of the muscle fibers) is used at times to estimate $F_o^M$.[125] When $A^M$ is used to estimate $F_o^M$, a value for muscle stress is assumed. And indeed, *muscle stress*, or "specific tension" ($F_o^M/A^M$), may vary among slow and fast muscle tissue, though the topic is controversial.[41,53,56,57,119,126] However, muscle stress does not have to be employed to formulate a muscle model (e.g., as shown here), since force, not $A^M$, is the quantity of interest. If muscle stress should be used, I believe values from single-fiber experiments (ca. 350 kPa)[112,119,127] would be more reliable than values from whole, multifibered muscle preparations because in the latter (1) some fibers may be inactivated, (2) pennation causes less (tendon) force to be measured than the muscle develops (see Section IV.H), and (3) the experimental paradigm for estimating peak isometric muscle force is flawed when tendon (either internal or external) is included in the preparation (see Section IV.C).

The optimal muscle fiber pennation angle $\alpha_o$ is a candidate for elimination. $\alpha_o$ is less

than 15° in most of those human muscles in which it has been measured, and these amounts of pennation are expected to barely affect the static and dynamical properties of the musculotendon actuator (see Section IV.H).[41-45] For clarity, unless otherwise noted, the discussion below assumes $\alpha_o = 0$.

When each of many mixed fiber-type muscles is to be described by a *SISO* model, it may be reasonable to assume that normalized maximum shortening velocity ($1/\tau_c \equiv v_m/L_o^M$) is muscle-independent. Assuming that fibers do not develop compressive forces (however, see Edman[73]), the reason $\tau_c$ can be assumed to be muscle-independent is that a fully activated mixed muscle will exert tension until the maximum shortening velocity of the fastest muscle fiber is reached.[128] When modeling mixed muscles, therefore, it seems reasonable to assume that the velocity-axis intercept at a(t) = 1 corresponds to the maximum shortening velocity $v_m$ of fast muscle tissue, which at 37°C is about $10L_o^M \cdot s^{-1}$.[57,111-114,118,128,129] Thus $1/\tau_c \approx 10 \cdot s^{-1}$, or $\tau_c \approx 0.1 \cdot s$, can be assumed for all mixed muscles.

To conclude, for mixed muscles only two rather than four muscle-specific parameters are needed to determine the static and dynamical properties of a specific muscle: $F_o^M$, peak isometric active muscle force and $L_o^M$, optimal muscle fiber length, since $\alpha_o \approx 0$ and $\tau_c \approx 0.1 \cdot s$. For highly pennated muscles, another parameter is required: $\alpha_o$, optimal muscle fiber pennation angle. And still another for muscles with very different normalized maximum shortening velocities: $\tau_c$, the time-scaling parameter (reciprocal of the normalized maximum shortening velocity of a muscle (see Equation 3).

# III. PROPERTIES AND MODELS OF TENDONS

## A. PROPERTIES OF TENDONS

Tendon, as defined in this review, consists of a portion external to muscle (i.e., the *external tendon*), and a portion internal to muscle (i.e., the aponeurosis of the muscle, called the *internal tendon*) (see Figure 1). Data suggest that the same strain is experienced throughout internal and external tendon.[37,39] (*Tendon strain* $\varepsilon^T$ is defined by the amount of tendon stretch relative to its resting, or slack length, i.e., $\varepsilon^T \equiv \Delta L^T/L_s^T = (L^T - L_s^T)/L_s^T$, where $L_s^T$ is the length on elongation at which tendon just begins to develop force. $L_s^T$ is called *tendon slack length* in this review.) It is also convenient to assume that the material (stress-strain) properties of external and internal tendon are the same.[37,39] (*Tendon stress* $\sigma^T$ is defined by the ratio of tendon force $F^T$ to tendon cross-sectional area $A^T$, i.e., $\sigma^T = F^T/A^T$.) For all parts of a tendon to experience the same strain, therefore, each must experience the same stress. For stress to be the same throughout the internal tendon, the cross-sectional area of the internal tendon must increase with proximity to the external tendon, assuming internal tendon force increases with proximity to the external tendon (refer to Figure 1). If all these assumptions should be fulfilled, then the aponeurosis, to which each muscle fiber attaches, would stretch by the same amount. Thus all muscle fibers would change length by the same amount. Many of these assumptions on the relation between muscle fibers and tendon have not been experimentally verified.

Though tendon properties are complex.[130] one important property relevant to coordination studies is its *stress-strain relation* ($\sigma^T$ vs. $\varepsilon^T$ curve) (see Figure 9A). The tendon tangent modulus of elasticity (i.e., the slope of the tendon stress-strain curve, $d\sigma^T/d\varepsilon^T$) increases with strain at low strains (the *toe region*), and then is constant (the *linear region*) at higher strains until failure, which occurs at about 10% strain and 100 MPa.[131-133] Data from many studies show directly, or suggest to me through analysis, that (1) the tendon tangent modulus in the linear region is (nominally) 1.2 GPa (range: 0.6 to 1.7 GPa), and (2) the linear region begins when tendon is stretched to 2% (range: 1.5 to 4%), or stressed to 16 MPa (range: 5 to 30 MPa).[39,131-142] However, the stress-strain response can be both short and long time-history dependent.[130,143] For instance, tendon must be stretched to consecutively longer lengths dur-

ing the first few cycles of application of repetitive cyclic loads in order to develop a small stress (e.g., 1 MPa),[144] and exercise can increase the tendon tangent modulus in the toe region.[135-137] On the other hand, the tendon stress-strain response appears to be independent of strain rate during locomotion.[134,138,140,142] Finally, when tendon shortens at physiological rates, it loses 6 to 11% of its energy.[138,142]

## B. MODELS OF TENDON

Tendon is assumed to be elastic or viscoelastic in almost all models used to study coordination, and, in some, its elasticity (or the combined elasticity of muscle and tendon) is assumed to be linear as well.[15,145-147] In the model developed here, tendon is assumed to be elastic, though if it should be assumed to be viscoelastic, musculotendon dynamics would still remain second-order, and the analysis techniques employed below would also remain applicable. In many models tendon elasticity is combined with the elasticity of muscle (i.e., muscle SEE), and this overall musculotendon elasticity is defined and referred to as the SEE (see Section II.B). Expressions and parameters used to specify this overall musculotendon elasticity are typically based on studies of "whole muscle", where some or all of the muscle aponeurosis is included in the "muscle" preparation and, at times, some or all of the external tendon as well.[29-31,70,90,111,148-150] As discussed earlier, I prefer to ascribe all series elasticity to (internal and external) tendon.

To model many tendons having unknown force-length ($F^T$ vs. $L^T$) curves, I favor the scaling of a *generic force-strain curve* ($\tilde{F}^T$ vs. $\varepsilon^T$ curve) by two parameters specific to an individual musculotendon actuator (i.e., peak active muscle force $F_o^M$ and tendon slack length $L_s^T$). A generic force-strain curve can be formulated by making two assumptions. First, a nominal, tendon-independent stress-strain relation is assumed based on the material properties of tendon (see above and Figure 9A). Second, the strain in tendon when its force equals peak isometric muscle force $F_o^M$ (call this strain $\varepsilon_o^T$) is assumed to be musculotendon-independent. The corresponding tendon stress will also be musculotendon-independent (call this stress $\sigma_o^T$) (see Figure 9A; $\sigma^T = \sigma_o^T = 32$ MPa when $\varepsilon^T = \varepsilon_o^T = 0.033$, which occurs when $F^T = F_o^M$). An implication of these two assumptions is that the ratio of tendon cross-sectional area to muscle physiological cross-sectional area is musculotendon-independent. Unfortunately, there are only scant data in direct support of this suggestion.[123,151,152]

Once $\varepsilon_o^T$ is assumed and $\sigma_o^T$ is specified, the generic force-strain ($\tilde{F}$ vs. $\varepsilon^T$) curve can be found from the stress-strain curve of tendon by using $\sigma_o^T$ to normalize stress (compare Figure 9A with Figure 9B). It is helpful to recognize that (1) *normalized tendon stress* $\tilde{\sigma}^T$ is equal to *normalized tendon force* $\tilde{F}^T$ (see Figure 9B) and (2) tendon strain $\varepsilon^T$ is a normalized quantity related to a normalized tendon length (i.e., $\varepsilon^T = [L^T - L_s^T]/L_s^T = [L^T/L_s^T] - 1$). Thus, the generic force-strain ($\tilde{F}^T$ vs. $\varepsilon^T$) curve is dimensionless and equals the normalized stress-strain ($\tilde{\sigma}^T$ vs. $\varepsilon^T$) curve (see Figure 9B). To obtain the fl curve of a specific tendon from the generic force-strain curve, $\tilde{F}^T$ is scaled by $F_o^M$, since $F^T = \tilde{F}^T \cdot F_o^M$, and $\varepsilon^T$ is scaled by $L_s^T$, since $L^T = (\varepsilon^T + 1) \cdot L_s^T$.

The obvious question is what should $\varepsilon_o^T$ and $\sigma_o^T$ be? Data from many studies suggest that an appropriate (nominal) value for $\varepsilon_o^T$ is 3.3% (range: 2 to 9%), corresponding to a nominal value for $\sigma_o^T$ of 32 MPa (range: 14 to 84 MPa).[8,36-39,142,153-155] The values of $\sigma_o^T = 32$ MPa and $\varepsilon_o^T = 3.3\%$ also seem reasonable given the following perspective. Since the highest force expected in tendon is 1.3 to $1.8F_o^M$ (i.e, corresponding to a fully activated muscle that is being stretched), and since tendon fails at about 112 MPa and 10% strain, these values for $\sigma_o^T$ and $\varepsilon_o^T$ give a safety factor of 1.9 to 2.7 times for tendon failure (i.e., tendon fails, nominally, when its force is $3.5F_o^M$; see Figure 9B).[152] However, tendon properties, and specifically the stress and strain corresponding to $F_o^M$, may well differ among actuators, especially since tendon does rupture.[156] Nevertheless, the approach to the following analysis would still be valid; only a trivial parameter change would have to be invoked to make tendon more or less compliant.

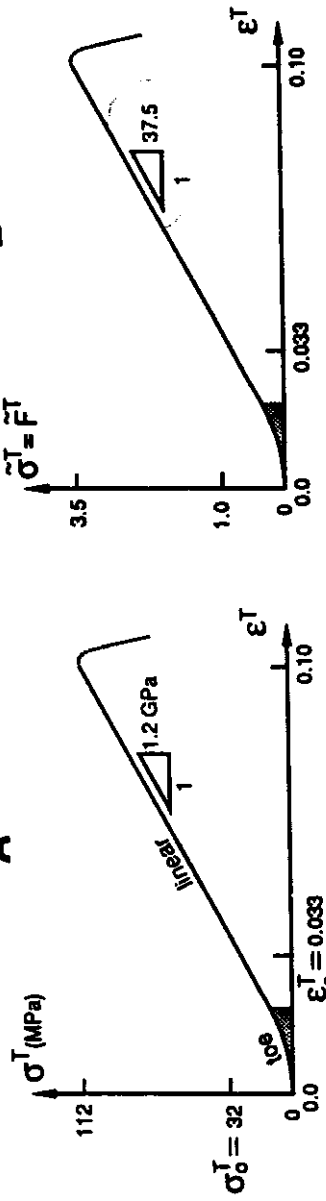


FIGURE 9. Material properties of tendon. (A) Nominal stress-strain curve ($\sigma^T$ vs. $\varepsilon^T$ curve). Tendon is more compliant in the *toe region* than in the *linear region*, where its tangent modulus is 1.2 GPa. The strain in tendon when $F^T = F_o^M$ is defined as $\varepsilon_o^M$ (nominally, $\varepsilon_o^T$ = 0.033). $\sigma_o^T$ is the stress in tendon when $F^T = F_o^M$ (nominally $\sigma_o^M$ = 32 MPa). (B) Generic, dimensionless force-strain curve ($\tilde{F}^T$ vs. $\varepsilon^T$ curve), which is also the normalized stress-strain curve. $\tilde{F}^T$ is the force in tendon relative to $F_o^M$ (i.e., $\tilde{F}^T = F^T/F_o^M$). $\tilde{\sigma}^T$ is tendon stress normalized by $\sigma_o^T$ ($\tilde{\sigma}^T \equiv \sigma^T/\sigma_o^T$). Defining $A^T$ to be the cross-sectional area of tendon, $\tilde{\sigma}^T = \tilde{F}^T$, since $\tilde{\sigma}^T = \sigma^T/(\sigma_o^T = \sigma^T/(F_o^M/A^T) = F^T/F_o^M = \tilde{F}^T$. Tendon strain $\varepsilon^T$ is defined by the amount of tendon stretch relative to its length. i.e., $\varepsilon^T \equiv \Delta L^T/L_s^T = (L^T - L_s^T)/L_s^T$, where $L_s^T$ is the length on elongation at which tendon just begins to develop force (called *tendon slack length*).

Because tendon is very compliant at low stress, estimates of tendon strain at low stress are poor and contribute to the poor estimates of $\varepsilon_o^T$, as evident by the wide range in $\varepsilon_o^T$ given above. For instance, as mentioned above, the strain at which stress is barely detectable increases on repetitive loading of the tendon.[144] Since there will be very little energy stored at these strains where stress is barely detectable (i.e., at strains up to 3%), my preference is to account for these uncertainties in strain by assuming that they are just uncertainties in estimation of tendon length at rest (i.e., tendon slack length $L_s^T$). With this approach, the stress-strain curve can be specified with much more confidence (e.g., see Figure 9A), and the dimensionless force-strain relation (e.g., see Figure 9B) may have more validity.

In summary, assuming that the stress-strain property is tendon-independent, as well as the strain in tendon when its force is $F_o^M$, then only one parameter is specific to each tendon. That parameter is the length on elongation at which it just begins to develop force (i.e., *tendon slack length*, $L_s^T$). Obviously, models could more accurately replicate the detailed and specific properties of each tendon if more complexity in model structure and more tendon-specific parameters were allowed. For simplicity, I feel that a constrained model of tendon is currently warranted when many tendons need to be modeled (e.g., in studies of coordination).

To conclude, tendon can be defined by a generic dimensionless force- (or dimensionless stress-) strain curve that is musculotendon-independent (see Figure 9B). Only two parameters are needed to scale this curve to obtain the force-length curve ($F^T$ vs. $L^T$ curve) of a specific tendon: $L_s^T$, tendon slack length and $F_o^M$, peak isometric active-muscle force. Notice that only one of these parameters is tendon-specific ($L_s^T$); the other ($F_o^M$) is muscle-specific.

# IV. PROPERTIES AND MODELS OF MUSCULOTENDON ACTUATORS

## A. THE MUSCULOTENDON ACTUATOR: WHY MUSCLE AND TENDON FUNCTION AS ONE ENTITY

Though muscle and tendon can be studied in isolation and their individual properties found, muscle and tendon function together. It is their integrated function that defines the properties of the musculotendon actuator. Indeed, the interaction of muscle and tendon has long been known. For example, muscle physiologists, including Hill, recognized that the determination of the properties of the contractile apparatus of muscle-tissue requires either the elimination of the series elasticity from the preparation (regardless of whether the elasticity resides in muscle, tendon, or the experimental apparatus) or, if series elasticity cannot be eliminated experimentally, its effect to be "subtracted" from the observations.[29,31]

Not only do muscle and tendon work together as an actuator (see Figure 10A), but they work together with the dynamics of the body segments. The reason interaction with the body segments occurs is that the force generating capability of an actuator is affected by its length $L^{MT}$ and velocity $v^{MT}$, which depend on the position and motion of the body segments. And body-segmental kinematics, in turn, depend on the force $F^T$ of each actuator. Thus muscle, tendon, and body segments constitute a coupled, multiple-input multiple-output (MIMO) feedback system (see Figure 10A).

This section will focus on only the properties of the musculotendon actuator: the properties of the complete MIMO system are not reviewed. Furthermore, tendon interacts with only the contraction process of the muscle tissue (e.g., see Figures 4 and 6); tendon has no interaction with the muscle activation process (see Figures 4 and 7) because activation is assumed to be uncoupled from the subsequent mechanical events. The combined function of tendon and muscle contractility is specified by their integrated dynamics (see Figure 10B). Notice that musculotendon length $L^{MT}$, velocity $v^{MT}$, and force $F^T$ affect only musculotendon contraction dynamics (see Figure 10B). Thus, musculotendon contraction dynamics will be emphasized and analyzed separately from activation dynamics.

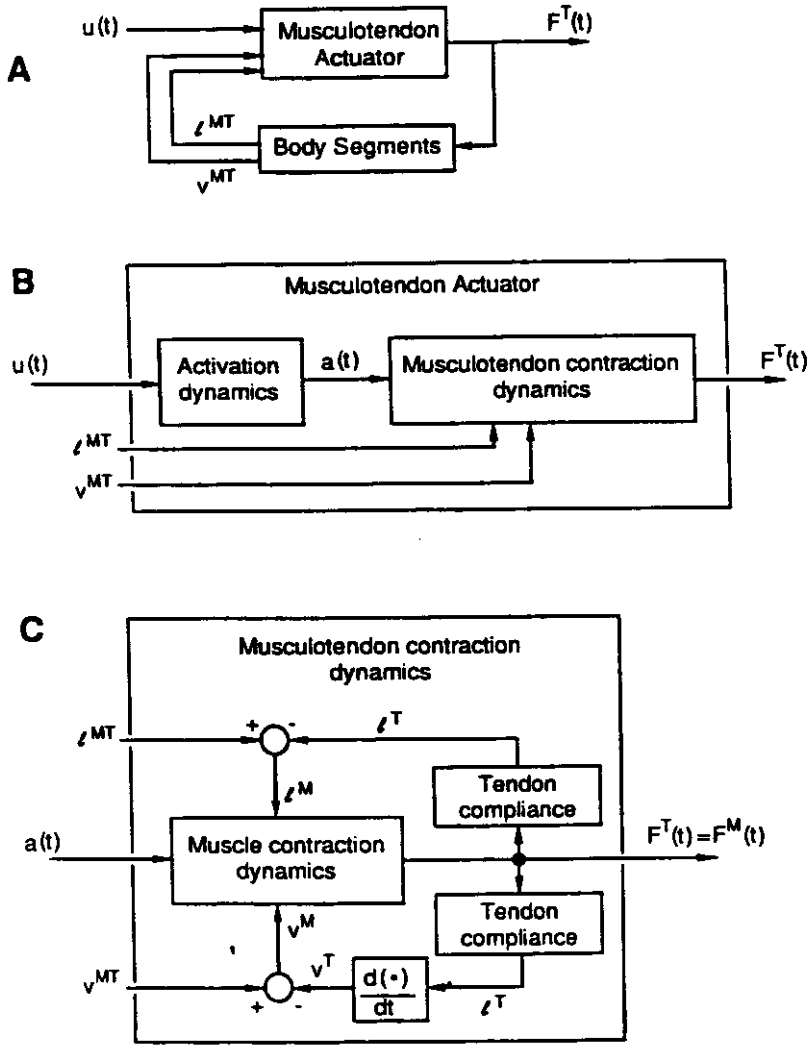


FIGURE 10. Block diagram to show the interaction of tendon and muscle in the generation of tendon force $F^T$. Tendon force equals muscle force $F^M$ because muscle fibers are assumed to be fusiform. (A) Diagram to show that musculotendon actuators work together with the body segments as a system to generate the forces that propel the body. (B) The dynamics of an actuator are composed of *activation dynamics* and *musculotendon contraction dynamics*. Notice that activation and musculotendon contraction are assumed to be uncoupled, and that actuator length $L^{MT}$ and velocity $v^{MT}$ affect only musculotendon contraction dynamics. Musculotendon contraction represents the integrated dynamical process of muscle and tendon working together. (C) Musculotendon contraction dynamics is given by the interaction of muscle contraction dynamics and tendon compliance. Notice that muscle contraction is influenced by muscle fiber length $L^M$ and velocity $v^M$ (i.e., the flv relation of muscle). Fiber length and velocity do not have a fixed relationship to actuator length $L^{MT}$ (origin to insertion distance) and velocity $v^{MT}$ because tendon has compliance and changes length as force changes. The trajectory of force output $F^T(t)$ is given by the input trajectories $L^{MT}(t)$, $v^{MT}(t)$, and a(t), where a(t) is given by the neural input trajectory u(t) (see *activation dynamics* in B).

The understanding of musculotendon contraction demands knowledge of how tendon compliance affects the dynamics. When tendon compliance is high, force output causes significant feedback onto the muscle fiber force-generating process (see Figure 10C). Notice that feedback exists because muscle fiber length $L^M$ and velocity $v^M$ are not mere reflections of actuator length $L^{MT}$ and velocity $v^{MT}$, but instead differ by the length of tendon $L^T$ and its velocity $v^T$. For example, suppose a musculotendon actuator should be lengthened by $\Delta L^{MT}$ and held there. In a compliant tendon actuator, muscle fibers would have to lengthen only a little in comparison to $\Delta L^{MT}$. The reason is that the highly compliant tendon would stretch a lot, and this stretch, not muscle stretch, would accommodate the stretch imposed on the actuator.

Highly compliant tendons, through the effects of tendon length and velocity (see Figure 10C), can also cause the velocity of the musculotendon actuator $v^{MT}$ to be *opposite* in direction to the velocity of its muscle fibers $v^M$. That is, at times, the origin-to-insertion distance of an actuator can lengthen while its muscle fibers shorten, or shorten while its muscle fibers lengthen. The exact conditions mitigating opposition between muscle fiber and actuator motion are important because a mechanism commonly hypothesized for efficient force production is that activated muscle fibers stretch before they shorten.[84,85,157-159] However, muscle fiber length is rarely measured directly; instead, musculotendon length is measured. Thus the assumption that changes in muscle fiber length mimic changes in musculotendon length may be invalid, especially for highly compliant actuators, and demands careful scrutiny.[5,8]

The question is, of course, when should tendon compliance be considered high? A generic, dimensionless model of the actuator facilitates answering this question because dimensionless musculotendon parameters, which define the properties of the actuator, can be found.

## B. THE DIMENSIONLESS MUSCULOTENDON ACTUATOR: FORMULATION AND DEFINITION OF ITS PARAMETER

From the tendon model and the SISO-muscle model developed previously, an individual actuator can be modeled by specifying five parameters: one tendon-specific parameter (tendon slack length [$L_s^T$]), and four muscle-specific parameters (peak isometric muscle force [$F_o^M$], optimal muscle-fiber length ($L_o^M$), optimal muscle-fiber pennation angle ([$\alpha_o$]), and the time-scaling parameter derived from the maximum shortening velocity of muscle ([$\tau_c$]).

Since three physical quantities are associated with actuator dynamics (force, length, and time), a dimensionless model generic among all actuators can be formulated. Choosing $F_o^M$, $L_o^M$, and $\tau_c$ as scaling parameters for force, length, and time, respectively, and assuming that pennation is zero for simplicity, the model has only one parameter. This one dimensionless parameter is tendon slack length, normalized by optimal muscle fiber length, and is defined to be $\tilde{L}_s^T \equiv L_s^T/L_o^M$.

In such a dimensionless formulation, therefore, the dimensionless properties of any actuator are given by only the ratio of tendon slack length to muscle fiber length $\tilde{L}_s^T$. To find the absolute properties of a specific actuator, the dimensionless properties are scaled by $F_o^M$, $L_o^M$, and $\tau_c$. Since activation dynamics is assumed to be unaffected by muscle fiber length or tendon slack length, $\tilde{L}_s^T$ has no effect on activation dynamics. The emphasis below is therefore on how $\tilde{L}_s^T$ affects musculotendon contraction dynamics.

What are realistic values of this ratio $\tilde{L}_s^T$? An estimate of actuator $\tilde{L}_s^T$ can be obtained from measurement of the length of its muscle-fibers ($L_o^M$) and its origin-to-insertion distance (i.e., $L_o^M + L_s^T$). Table 1 lists $\tilde{L}_s^T$ for some human and cat lower-extremity muscles. Notice that in both human and cat muscles the trend is for $\tilde{L}_s^T$ to be smaller in proximal muscles, and that cat muscles generally have lower ratios than human muscles. However, for other species, specifically animals with long extremities,[140,155] $\tilde{L}_s^T$ will be higher than even the values listed in Table 1 for human muscles. Using data of human upper-extremity muscle fiber lengths,[123,124] I estimate the heads of the biceps and triceps muscles to have ratios between 1

**TABLE 1**
**Tendon Slack Length to Muscle Fiber Length Ratio ($\tilde{L}_s^T$) for Human and Cat Lower-Extremity Muscles**

| | Human[a] ($\tilde{L}_s^T \equiv L_s^T/L_o^M$)[c] | Cat[b] ($\tilde{L}_s^T \equiv L_s^T/L_o^M$)[c] |
|---|---|---|
| Plantarflexors | | |
| Soleus | 11 | 2 |
| Gastrocnemius | 9 | 5 |
| Others | 7 | 6 |
| Dorsiflexors | 3 | 2 |
| Quadriceps | | |
| Vasti | 3 | 3 |
| Rectus femoris | 5 | 4 |
| Hamstrings | | |
| Semitendinosus | 2 | 1 |
| Semimembranosus/biceps (long) | 7 | 2 |
| Hip uniarticular muscles | 0.2[d] | 1 |

[a] Muscle fiber lengths ($L_o^M$) were obtained from Bobbert et al.,[8] Alexander and Vernon,[44] Wickiewicz et al.,[122] and Huijing.[160]

[b] Muscle fiber lengths were obtained from Rack and Westbury,[39] Walmsley and Proske,[91] Sacks and Roy,[121] and Roy et al.[161a]

[c] $L_s^T$ was calculated by subtracting $L_o^M$ from the origin-to-insertion distance of the musculotendon actuator, estimated from apatomical measurements.

[d] These ratios of $\tilde{L}_s^T$ were obtained from Hoy et al.[161]

and 2, and the long forearm muscles, which extend and flex the wrist and fingers, to have ratios between 3 and 8. Thus the trend for proximal muscles to have lower tendon slack-length to muscle fiber-length ratios ($\tilde{L}_s^T$) seems also to exist in the upper extremity.

Since an actuator that has a ratio of $\tilde{L}_s^T = 1$ functions very differently than one having a ratio of $\tilde{L}_s^T = 10$ (see below), *stiff and compliant actuators* can be defined. Because tendon is elastic, tendon compliance is proportional to tendon slack length. Thus, an actuator can be said to be highly compliant when it has a $\tilde{L}_s^T$ so large as to significantly affect its properties (e.g., $\tilde{L}_s^T = 10$). Similarly, a very stiff actuator is one with a $\tilde{L}_s^T$ so small as to have no significant effect (e.g., $\tilde{L}_s^T = 1$). Importantly, an actuator is not necessarily compliant just because it has a compliant or long tendon. Whether an *actuator* is compliant depends on the *ratio* of its tendon slack length to muscle fiber length ($\tilde{L}_s^T$). Though I refer to actuators as being compliant or stiff in the following discussion, and as having long or short tendons, I am actually referring to actuators that have high or low ratios of tendon slack length to muscle fiber length.

## C. THE DIMENSIONLESS MUSCULOTENDON ACTUATOR: STATIC PROPERTIES

How is the fl relation of the musculotendon actuator affected by the ratio of tendon slack length to muscle fiber length $\tilde{L}_s^T$? One important, though uninteresting effect is that the actuator has to be longer than the length of muscle fibers by an amount equal to the tendon slack length $\tilde{L}_s^T$ in order to sustain force. Otherwise the tendon is slack and muscle fibers are too short to generate force (i.e., for $F^T = F^M > 0$, $L^{MT} > L_s^T + 0.5L_o^M$, Figure 5A, or, equivalently, for $\tilde{F}^T = \tilde{F}^M > 0$, $\tilde{L}^{MT} > \tilde{L}_s^T + 0.5$, Figure 8A). Refer to Figure 11 for the definitions of *dimensionless lengths* (e.g., $\tilde{L}^{MT}$) and *dimensionless forces* (e.g., $\tilde{F}^T$).

Of more interest is the amount by which an actuator must be stretched, beyond that needed to stretch its muscle fibers, to accommodate an increase in force. Figure 12 shows how tendon stretch ($\Delta\tilde{L}^T$) of a somewhat stiff actuator ($\tilde{L}_s^T = 3$) or a very compliant actuator

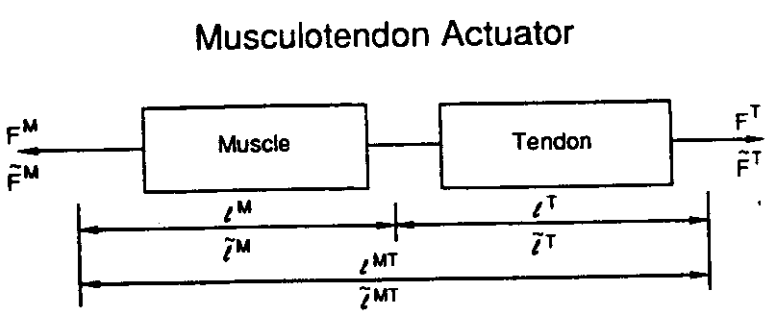


FIGURE 11. Definition of muscle, tendon, and musculotendon (actuator) forces, lengths, and velocities. Muscle is assumed to be fusiform ($\alpha_o = 0$). All forces ($F^M$, $F^T$) and lengths ($L^M$, $L^T$, $L^{MT}$) can be normalized by peak active muscle force ($F^M_o$) and optimal muscle fiber length ($L^M_o$), respectively, to form dimensionless forces ($\tilde{F}^M$, $\tilde{F}^T$) and lengths ($\tilde{L}^M$, $\tilde{L}^T$, $\tilde{L}^{MT}$). All velocities ($v^M$, $v^T$, $v^{MT}$) can be made dimensionless by normalizing with respect to the muscle maximum shortening velocity ($v_m = L^M_o/\tau_c$) (e.g., $\tilde{v}^{MT} \equiv d\tilde{L}^{MT}/d\tau = dL^{MT}/dt \cdot [\tau_c/L^M_o] = v^{MT}/v_m$). Parameters can also be made dimensionless: the ratio of tendon slack length to optimal fiber length is given by $\tilde{L}^T_s \equiv L^T_s/L^M_o$, and peak active force $F^M_o$ and optimal fiber length $L^M_o$ become one when normalized.

($\tilde{L}^T_s = 15$) affects the shape of the actuator fl curve (i.e., $\tilde{F}^T$ vs. $\tilde{L}^{MT}$ curve), assuming the muscle to be fully activated a(t) = 1. For the stiff actuator, the muscle fl curve is distorted little (see Figure 12A), but the compliant actuator causes much distortion (see Figure 12B). Notice that the range of lengths where the compliant actuator operates on the ascending region of the fl curve of its muscle fibers is almost 2 times the range of the stiff actuator (see Figure 12, compare "bars"). In fact, for the model being used here, the amount of stretch in tendon when $\tilde{F}^T = 1$ (i.e., when $F^T = F^M_o$) is (see Figure 9B)

$$\Delta\tilde{L}^T = 0.033 \cdot \tilde{L}^T_s;\ \tilde{F}^T = 1 \text{ or } F^T = F^M_o \tag{7}$$

Thus the actuator length range associated with muscle fibers operating on the ascending region of their fl curve is

$$\left(\Delta\tilde{L}^{MT}\right)_{F^T:o\to F^M_o} = \left(\Delta\tilde{L}^{M}\right)_{F^T:o\to F^M_o} + \left(\Delta\tilde{L}^{T}\right)_{F^T:o\to F^M_o} = 0.5 + \left(0.033 \cdot \tilde{L}^T_s\right) \tag{8}$$

In absolute quantities, Equation 8 becomes

$$\left(\Delta L^{MT}\right)_{F^T:o\to F^M_o} = 0.5L^M_o + \left(0.033\ L^T_s\right) \tag{9}$$

To conclude, because of tendon stretch, very long tendon actuators (e.g., $L^T_s = 15L^M_o$) need to be stretched beyond what muscle fibers alone would have to be to accommodate peak isometric force $F^M_o$ (see Figure 12 and Equation 9).

Next I would like to caution readers that fl curves of "muscle tissue" reported in the literature may often be erroneous. Before I explain how such errors can arise, remember how experiments are performed to estimate the fl curve of a muscle. The muscle, with some or all of its tendon attached, is held isometric and fully activated, and tendon force above the baseline is measured. An isometric fl curve is constructed from such measurements. The curve so constructed is the fully activated actuator fl curve. The actuator is then put at the same musculotendon lengths as the fully activated actuator had been, and passive force is recorded. At

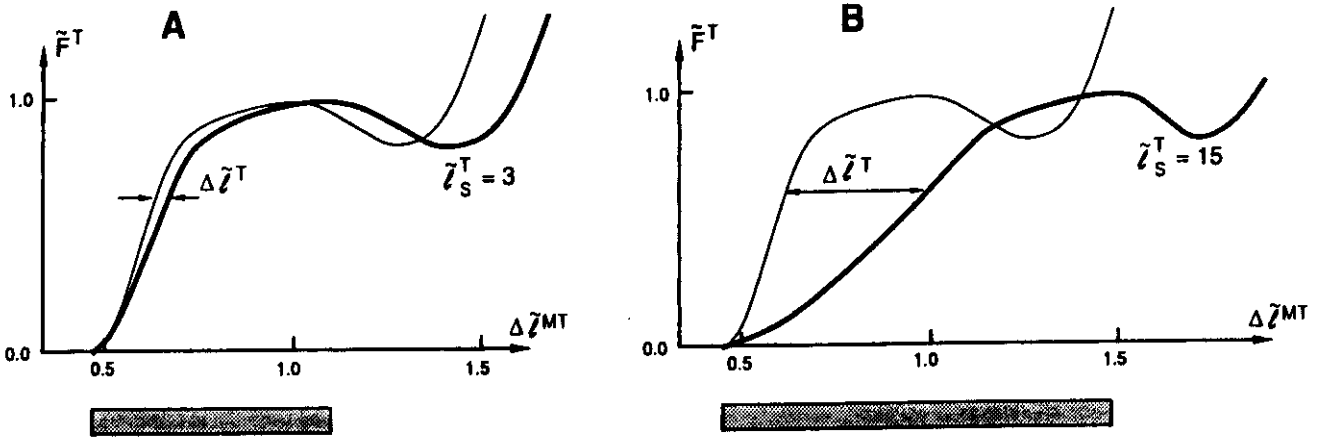


FIGURE 12. Isometric fl relation of a stiff tendon actuator (A, $\tilde{L}_s^T = 3$) and a compliant tendon actuator (B, $\tilde{L}_s^T = 15$) compared with the fl relation of a compliantless tendon actuator. The fl curve (thin line in A, B) of the compliantless tendon actuator is shaped exactly as the muscle fl curve, since tendon does not stretch. The fl curve of both the stiff and the compliant actuator (bold line in A, B) is a distortion of the muscle fl curve, especially in the compliant tendon actuator (B). $\Delta\tilde{L}^T$, the amount of stretch in tendon, causes the distortion. Notice that the length range of the actuator where its muscle fibers operate on the ascending region of their fl curve is much wider for the compliant than for the stiff tendon actuator (compare bars in A and B). For compliantless tendon actuators, the range is even less and would be the same as the muscle range (about 0.5). The actual length plotted $\Delta\tilde{L}^{MT}$ is the deviation of the length of the musculotendon actuator from tendon slack length, expressed dimensionlessly (i.e., $\Delta\tilde{L}^{MT} = \tilde{L}^{MT} - \tilde{L}_s^T$). Force is also expressed dimensionlessly, i.e., $\tilde{F}^T \equiv F^T/F_o^M$.

each musculotendon length, the measured passive force is subtracted from the measured fully activated force. The net force vs. the musculotendon length relation is called (putatively) the fl curve of the muscle.

To show that the fl curve obtained in this way can indeed be a misrepresentation of the "actual" fl curve of muscle, consider the following results of a simulation of such an experiment, where the preparation is assumed to be a very long tendon actuator (i.e., $\tilde{L}_s^T = 16$; see Figure 13). The simulated, passive fl curve of the actuator (bold dotted line) is subtracted from its fully activated fl curve (bold dashed line) to obtain the net force vs. the musculotendon length curve (bold solid line, *Estimated*). Notice that this (putative) fl curve of "active muscle" (bold solid line, *Estimated*) differs significantly from the actual fl curve of muscle used in the simulation (thin solid line, *Actual*). Importantly, peak muscle force is underestimated (solid circles), and the range of active muscle force generation is overestimated (compare the two bars). Also, the stretch minimally needed for the *actuator* to develop passive force (i.e., $\Delta L^{MT} = L_o^M$) is *less* than the stretch needed for the *actuator* to develop peak active force (i.e., $\Delta L^{MT} \approx 1.2L_o^M$), even though the simulation had *muscle* generate passive force only at lengths *longer* than that needed for *muscle* to develop peak active force.

The reason the estimated fl curve of the muscle fibers differs from the actual one is that muscle fibers are not at the same length when passive- and activated-muscle force measurements are made, even though the length of the musculotendon actuator is. The muscle fibers are at different lengths because tendon is stretched by unequal amounts due to the different forces in the tendon when the actuator is passive and activated. A correction for tendon stretch is thus necessary to accurately estimate the active fl curve of the muscle.[29,31] Unfortunately, the length of tendon free of the tendon clamp has rarely been reported; so corrections and comparisons among studies will be difficult to interpret. The length of tendon included in the preparation should be reported so that results of any given experiment can be reproduced. Finally, since peak active muscle force can be underestimated, muscle stress may also be underestimated. Such low estimates may explain the difference in the muscle stresses estimated from *in vivo* and *in vitro* muscle tissue experiments (see Section II.D).

These distortions will be most prominent when muscle is highly activated, as illustrated above, because high forces are then developed. The influence of tendon on the static properties of actuators will be much less when muscle fibers are submaximally activated (i.e., $a(t) < 1$) because the smaller forces in tendon will cause it to stretch less. Changes in muscle fiber length will then better match changes in musculotendon length.

## D. THE DIMENSIONLESS MUSCULOTENDON ACTUATOR: DYNAMIC PROPERTIES, GENERAL CONSIDERATIONS, AND DEVELOPMENT OF A LINEAR MODEL

Musculotendon actuator dynamics is second-order, and can be divided into two first-order processes (see Figure 10). Activation dynamics (one first-order process) has already been presented in dimensionless form (see Equation 6) and is unaffected by the ratio of tendon slack length to muscle fiber length ($\tilde{L}_s^T$). A dimensionless model for musculotendon contraction dynamics (the other first-order process) is developed next.[162]

In this and the next two sections, emphasis is given to the effects of $\tilde{L}_s^T$ on musculotendon contraction dynamics and how models of this dynamics can be applied to analyze the function of actuators during specific motor tasks. For example, does an actuator behave as a *spring* in one motor task, as a *dashpot* in another, and as a *CNS-controlled force generator* in still another?

### 1. Musculotendon Contraction Dynamics: Nonlinear Model

To assess actuator function in a motor task, a dimensionless dynamical model is developed. To develop the model, the dimensionless rate of change in tendon force $d\tilde{F}^T/d\tau$ must be

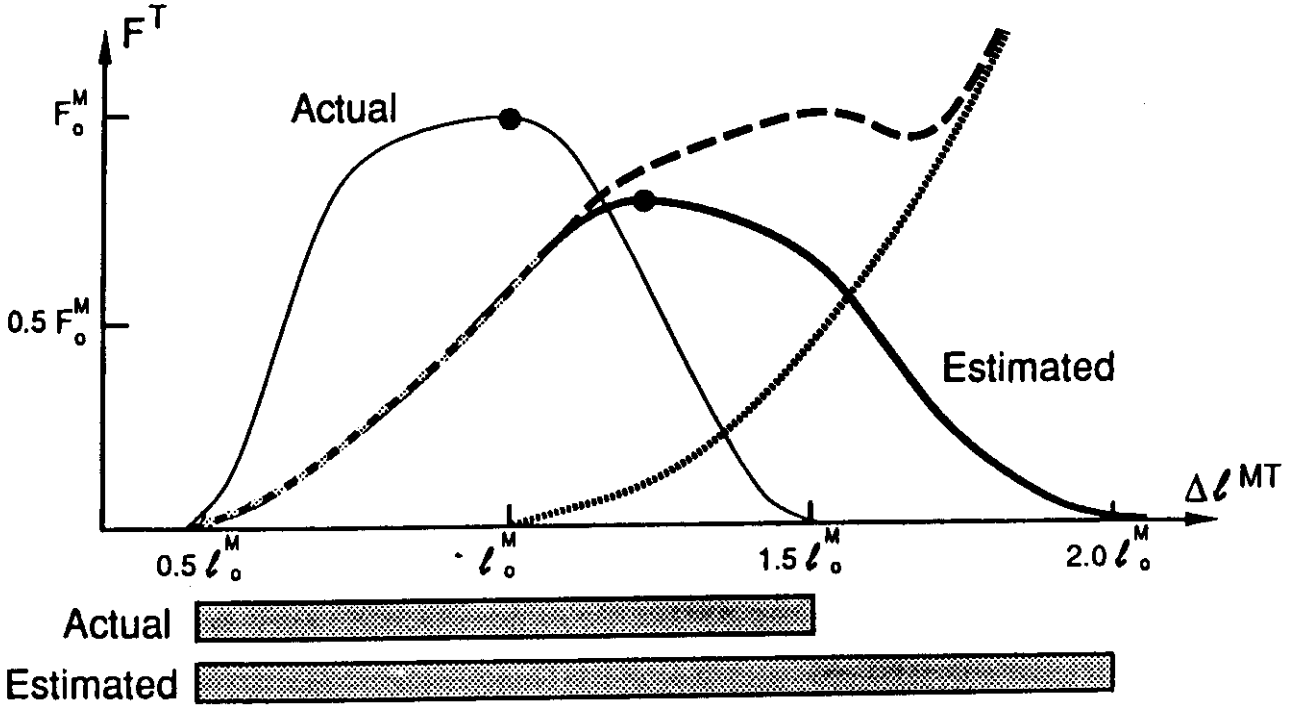


FIGURE 13. Computer simulation to show how the muscle fl curve can be inaccurately estimated when actuators have long tendons. The *estimated* fl curve of muscle (bold solid line) is obtained by subtracting the fl curve of the passive musculotendon actuator (bold dotted line) from the fl curve of the fully activated actuator (bold dashed line). The *actual* fl curve of muscle used in the simulation is the thin solid line. Notice how peak force is underestimated (compare filled circles), and how the range corresponding to active force generation is overestimated (compare the lengths of the "bars").

given in terms of the dimensionless state variables, which are tendon force $\tilde{F}^T = (\tilde{F}^T = F^T/F_o^M)$, musculotendon length $\tilde{L}^{MT}$ ($\tilde{L}^{MT} = L^{MT}/L_o^M$), and musculotendon velocity $\tilde{v}^{MT}$ [$\tilde{v}^{MT} \equiv d\tilde{L}^{MT}/d\tau = v^{MT}/(L_o^M/\tau_c)$] (see Figure 11 for definitions). First, however, let absolute stiffness and dimensionless stiffness of tendon be defined:

$$k^T \equiv \frac{d\,F^T}{d\,L^T} = \text{the } \textit{absolute tendon stiffness}, \text{ and}$$

$$\tilde{k}^T \equiv k^T \cdot \left(L_o^M/F_o^M\right) = \text{the } \textit{dimensionless tendon stiffness} \tag{10}$$

Notice that $\tilde{k}^T$ is proportional to $k^T$ by the ratio of optimal muscle fiber length to peak isometric muscle force (i.e., by $L_o^M/F_o^M$). It is easy to show from Equation 10 and the definition of $\tilde{F}^T$ and $\tilde{L}_s^T$ that

$$\tilde{k}^T = \left(\frac{d\,\tilde{F}^T}{d\,\varepsilon^T}\right) \cdot \frac{1}{\tilde{L}_s^T} \tag{11}$$

Notice that $d\tilde{F}^T/d\varepsilon^T$ is obtainable from the $\tilde{F}^T$ vs. $\varepsilon^T$ curve (see Figure 9B) and depends on $\tilde{F}^T$, which is the physical (state) variable of interest. Thus, dimensionless tendon stiffness $\tilde{k}^T$ depends on the current force $\tilde{F}^T$. It also follows from Equation 11 that *dimensionless tendon compliance*, defined as $1/\tilde{k}^T$, is proportional to $\tilde{L}_s^T$, and dimensionless tendon stiffness is inversely proportional to $\tilde{L}_s^T$.

The key to expressing dimensionlessly the contraction dynamics of an actuator is to first find the muscle fiber velocity for a given muscle force, fiber length, and activation using a Hill-type model (see Section II.B), then to sum this function for muscle fiber velocity with tendon velocity, and finally to recognize that the summed velocity is the velocity of the actuator. Since the flv relation of a muscle can be written as

$$\tilde{v}^M = f(\tilde{L}^M, \tilde{F}^M, a(\tau)) \tag{12}$$

and

$$\tilde{L}^M = \tilde{L}^{MT} - \tilde{L}^T = \tilde{L}^{MT} - (\tilde{L}_s^T + \tilde{F}^T/\tilde{k}^T)$$

$$\tilde{L}_s^T = \text{const.}$$

$$\tilde{F}^T = \tilde{F}^M \tag{13}$$

then with Equation 13 into Equation 12

$$\tilde{v}^M = f_1(\tilde{L}^{MT}, \tilde{F}^T, a(\tau)) \tag{14}$$

Recognizing that $d\tilde{F}^T/d\tau$ is proportional to tendon velocity $\tilde{v}^T$, which is the difference between musculotendon velocity $\tilde{v}^{MT}$ and muscle velocity $\tilde{v}^M$ (see Figure 11), then

$$\frac{d\tilde{F}^T}{d\tau} = \tilde{k}^T \cdot [\tilde{v}^{MT} - \tilde{v}^M] \tag{15}$$

From Equations 14 and 15, musculotendon contraction dynamics can be expressed dimensionlessly:

$$\frac{d\tilde{F}^T}{d\tau} = \tilde{k}^T \cdot \left[\tilde{v}^{MT} - f_1(\tilde{L}^{MT}, \tilde{F}^T, a(\tau))\right] \tag{16}$$

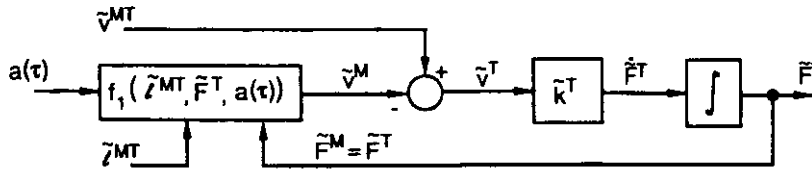


FIGURE 14. Block diagram of musculotendon contraction dynamics. Notice that activation $a(\tau)$, and musculotendon length $\tilde{L}^{MT}$, and velocity $\tilde{v}^{MT}$ are *inputs* to the musculotendon actuator. Force $\tilde{F}^T = \tilde{F}^M$ is the *output*.

In summary, Equation 16 is the contraction dynamics of the actuator expressed dimensionlessly, and the ratio of tendon slack length to muscle fiber length $\tilde{L}_s^T$ is the only actuator-specific parameter. Once $\tilde{L}_s^T$ is given, the *dimensionless* dynamics are specified. The *actual* dynamics of a specific actuator can be found by using $F_o^M$, $L_o^M$, $\tau_c$, and $L_o^M/\tau_c$ to scale all dimensionless force, length, time, and velocity variables, respectively. ($L_o^M/\tau_c$ is the maximum shortening velocity of muscle, $v_m$ ; see Equation 3.)

The dimensionless dynamics (i.e., Equation 16), when expressed as a block diagram (see Figure 14), shows that actuator length and velocity ($\tilde{L}^{MT}$ and $\tilde{v}^{MT}$) are *inputs* to the actuator, just as muscle activation $a(\tau)$ is. Thus, all three inputs interact and affect force generation $\tilde{F}^T$. Expectedly then, the actuator has at times been considered to act as a *spring*, where its force output $\tilde{F}^T$ depends only on its length $\tilde{L}^{MT}$, and at other times as a *dashpot* (or "viscous" element), where its force output depends only on its velocity $\tilde{v}^{MT}$, and still at other times as an *independent, CNS-controlled force generator*, where its force output depends only on its neural input $u(\tau)$ (equivalent to $a(\tau)$, after accounting for activation dynamics).[163,164]

To ascertain whether an actuator behaves like a spring, a dashpot, or an independent, CNS-controlled force generator, the dimensionless dynamics of the actuator must be known (e.g., Equation 16), $\tilde{L}_s^T$ must be given, and the frequency content of the input signals must be specified. However, only the frequency content of length $\tilde{L}^{MT}(\tau)$ and activation $a(\tau)$ must be known. The reason the frequency content of $\tilde{v}^{MT}(\tau)$ does not have to be specified is that it has a one-to-one correspondence to the frequency content of $\tilde{L}^{MT}(\tau)$ since $\tilde{v}^{MT}(\tau)$ is the dimensionless rate of change of $\tilde{L}^{MT}$ (i.e., $d\tilde{L}^{MT}/d\tau$).

## 2. Musculotendon Contraction Dynamics: Linear Model

To show how dimensionless dynamics can be employed to assess whether an actuator operates as a spring or a dashpot, for example, the dynamics given in Equation 16 will be simplified. Of course, for exactness, computer simulation can be used in lieu of the following analysis. Assume all muscle and tendon properties are linear (see Figure 15). Tendon stretch is assumed to be linear in tendon force (see Figure 15A), from which $\tilde{k}^T = 30/\tilde{L}_s^T$ follows. Muscle is assumed to have a fv curve that scales with $a(\tau)$ (see Figure 15B).[16] Reasons were given in Section II.B for why the velocity-axis intercept can be assumed to scale with $a(\tau)$. Another one is based on the fact that in mixed muscles, and perhaps in homogeneous muscles as well, when $a(\tau)$ is low, only muscle fibers slower than the fastest are recruited.[53,165,166] Since mixed muscles are the focus of the examples discussed below, and since slow fibers have a slower maximum shortening velocity than fast fibers, once again scaling the velocity-axis intercept seems justified.

Each of two cases will be analyzed to show how dimensionless dynamics can be used to assess whether an actuator functions as a spring or a dashpot. Muscle fiber movement is assumed to be restricted to the flat region of its fl curve in case 1 and to the ascending region in case 2 (see Figure 15C, dashed and solid lines, respectively). Also, in case 2, muscle fiber length $\tilde{L}^M$ is assumed to scale the fv curve (see Figure 15D), i.e, when $\tilde{L}^M < 1$, the velocity- and force-axis intercepts are assumed to be reduced proportionately with isometric force (compare points [a] and [b] in Figure 15C with lines [a] and [b] in Figure 15D).

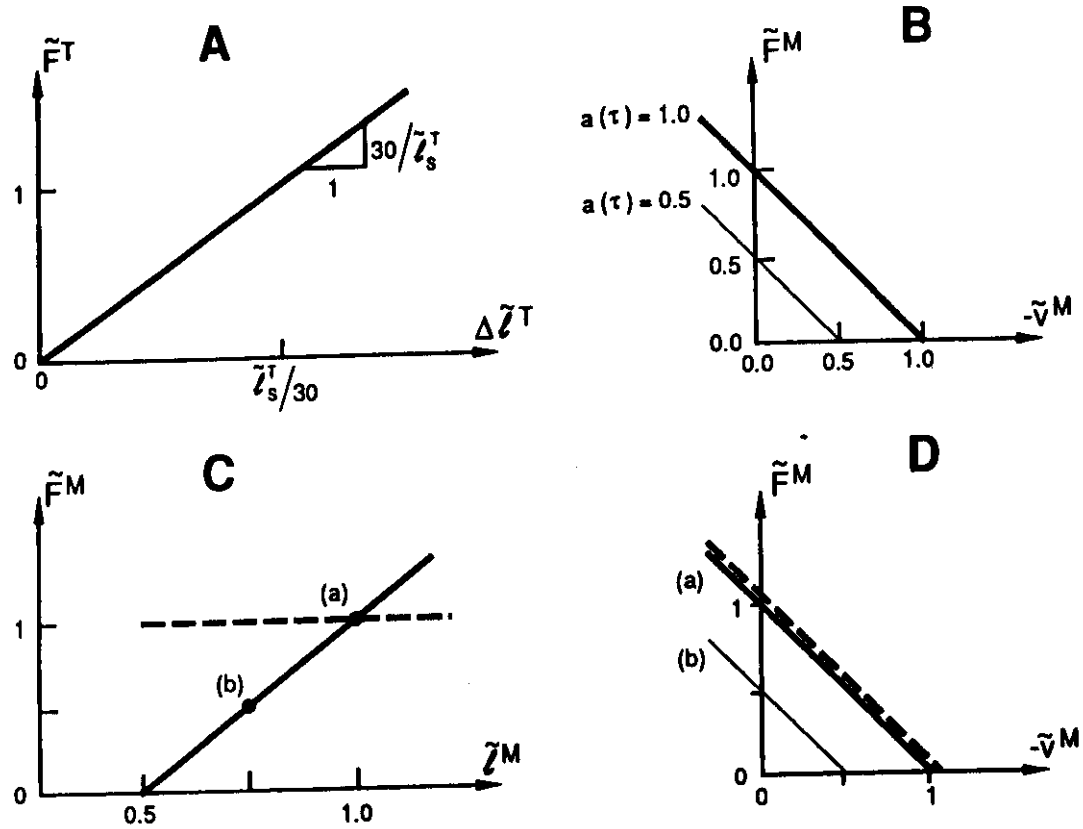


FIGURE 15. Linear model of muscle and tendon. (A) The dimensionless force vs. the tendon stretch curve ($\tilde{F}^T$ vs. $\Delta\tilde{L}^T$ curve) of tendon. Tendon is assumed to be stretched by an amount $L_s^T/30$ when its force equals peak active muscle force (i.e., when $F^T = F_o^M$, or $\tilde{F}^T = 1$, it is assumed that $\varepsilon^T = 1/30 = 0.033$; thus $\Delta\tilde{L}^T = \tilde{L}^T - \tilde{L}_s^T = \tilde{L}_s^T/30$). The slope represents the dimensionless stiffness of the tendon, defined as $\tilde{k}^T = k^T \cdot (L_o^M/F_o^M)$. Thus, $\tilde{k}^T = 30/\tilde{L}_s^T$. (B) The fv curve of muscle is assumed to scale with a(τ), i.e., both isometric force (ordinate-intercept) and no-load shortening velocity (abscissa-intercept) decrease with a(τ). (C) One case (case 1) assumes that the muscle fl curve is flat (dashed line); the other (case 2) that it is ascending (solid line). (D) The fv curve for case 1 is the same regardless of muscle length $\tilde{L}^M$ (bold dashed line). The fv curve for case 2 scales with muscle length $\tilde{L}^M$ (solid lines). Curve (a) in D (bold solid line) is the fv curve when $L^M = L_o^M$ and corresponds to point (a) in C. Curve (b) in D (thin solid line) is the fv curve when $L^M = 0.5L_o^M$ and corresponds to point (b) in C.

## E. MUSCULOTENDON CONTRACTION DYNAMICS WHEN MUSCLE OPERATES ON THE FLAT REGION OF ITS FL CURVE (CASE 1)

Actuator dynamics is first developed and analyzed, and then I will show how the dynamics can be utilized to study, for example, the function of hip actuators during walking. To develop the dimensionless dynamics when muscle operates on the flat region of its fl curve, recognize from Figure 15 that

$$-\tilde{v}^{M} = a(\tau) - \tilde{F}^{M} \tag{17}$$

and with Equation 17 into 15 the dynamics becomes (since $\tilde{F}^{T} = \tilde{F}^{M}$):

$$\frac{d\tilde{F}^{T}}{d\tau} + \left(\tilde{k}^{T}\right) \cdot \tilde{F}^{T} = \tilde{k}^{T} \cdot \left[\tilde{v}^{MT} + a(\tau)\right] \tag{18}$$

How an actuator operates can be found by expressing Equation 18 as a block diagram and analyzing its frequency response (see Figure 16). Notice from Figure 16A and the left side of Equation 18 that force develops with a lag with time constant $1/\tilde{k}^{T}$.

One way to view an actuator is as a force generator driven by errors in an activation-controlled velocity set-point. Figure 16A shows that force output $\tilde{F}^{T}$ depends on the sum of its lengthening velocity $\tilde{v}^{MT}(\tau)$ and its activation $a(\tau)$ or, equivalently, the difference between its shortening velocity and its activation. As long as the shortening velocity and the activation of an actuator differ, an error signal will be generated and, after a lag, force will develop that is proportional to this difference.

Another way to view an actuator is as a low-pass filter to activation $a(\tau)$ and a high-pass filter to actuator length $\tilde{L}^{MT}$, with both filters having the same cut-off frequency $\tilde{\omega}_c$ (see Figure 16B). For a frequency response analysis, recognize that $\tilde{v}^{MT}$ does not have to be considered as an independent input, since it is specified once $\tilde{L}^{MT}$ is specified (i.e., $\tilde{v}^{MT} = d\tilde{L}^{MT}d\tau$). Thus, when length $\tilde{L}^{MT}$ changes slowly, the actuator responds to musculotendon velocity and acts as a dashpot, since actuator gain to length $\tilde{L}^{MT}$ increases with frequency (see Figure 16B, left plot, $\tilde{\omega} < \tilde{\omega}_c$). For high-frequency changes in length, the actuator responds to musculotendon length and acts as a spring, since its gain is constant with frequency (Figure 16B, left plot, $\tilde{\omega} > \tilde{\omega}_c$). Similarly, the actuator responds directly to its activation when activation changes slowly, since its gain is then flat, and it responds to an integrated activation signal otherwise, since actuator gain falls at high frequencies (see Figure 16B, right plot). The dimensionless cut-off frequency $\tilde{\omega}_c$ of an actuator can be used, therefore, to assess how the actuator will respond to its inputs.

The *dimensionless cut-off frequency* of an actuator $\tilde{\omega}_c$ depends only on its tendon slack length to muscle fiber length ratio $\tilde{L}_s^T$. In fact, $\tilde{\omega}_c$ is inversely proportional to $\tilde{L}_s^T$ (i.e., $\tilde{\omega}_c = \tilde{k}^T = 30/\tilde{L}_s^T$; see Figure 16B). Thus one parameter $\tilde{L}_s^T$ of an actuator specifies its cut-off frequency $\tilde{\omega}_c$. For example, in the human lower extremity, many uniarticular hip actuators have short tendons ($0.01 < \tilde{L}_s^T < 1.0$) and operate on the flat region of their fl curves (see Table 1).[161] Thus, these actuators have high, dimensionless cut-off frequencies (i.e., $\tilde{\omega}_c > 30$).

Once the dimensionless cut-off frequency $\tilde{\omega}_c$ of an actuator is estimated from its parameter $\tilde{L}_s^T$, its *absolute cut-off frequency* ($\omega_c$ in rad/s) can be found by recognizing that $\tau_c$ scales frequency, since it scales time (i.e., $\omega = \tilde{\omega}/\tau_c$ and thus $\omega_c = \tilde{\omega}_c/\tau_c$). Thus, the absolute cut-off frequency of an actuator having only fast muscle tissue is expected to be $\omega = \tilde{\omega}_c/0.1$, since $\tau_c = 0.1$ s for fast muscle tissue (see Section II.D). A mixed muscle fiber-type actuator is also expected to have a cut-off frequency of $\omega_c = \tilde{\omega}_c/0.1$, since the maximum shortening velocity per unit length of a mixed muscle has been assumed to be equal to that of fast muscle tissue (i.e., their $\tau_c$ values have been assumed to be identical). For example, since $\tilde{\omega}_c > 30$ in human uniarticular hip muscles, and assuming the fiber composition of

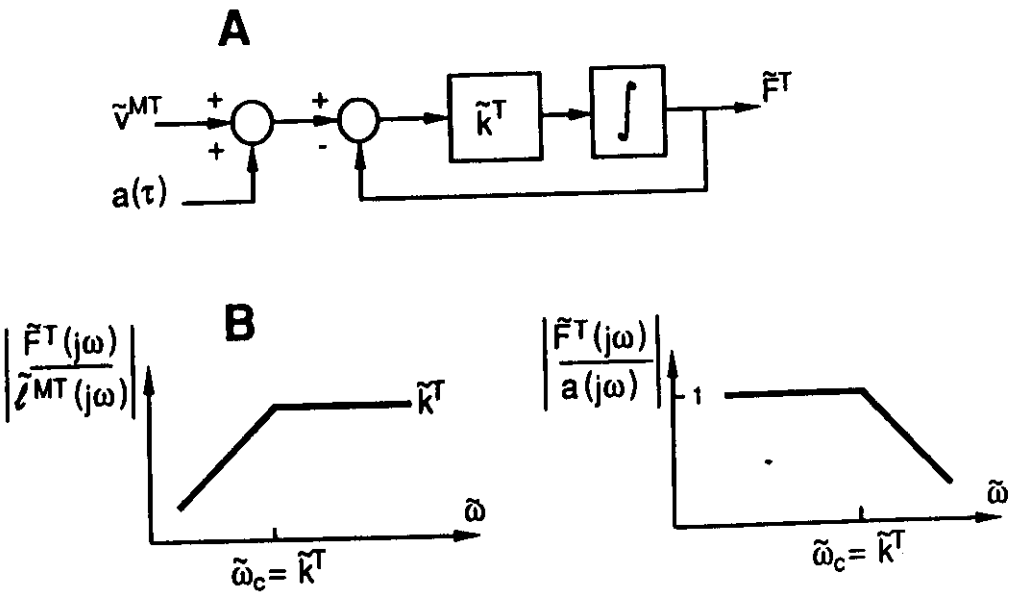


FIGURE 16. Block diagram (A) and dimensionless frequency response (B) of an actuator when its muscle fibers operate on the flat region of their fl curve (case 1). In A, the input is considered to be the actuator velocity $\bar{v}^{MT}$, but length $\bar{L}^{MT}$ can also be the input, since the two are related by $\bar{v}^{MT} = d\bar{L}^{MT}/d\tau$. In B, the left plot shows the frequency response (i.e., the I/O gain) of an actuator to length $\bar{L}^{MT}$, and the right plot to activation a(τ), i.e., how the amplification of force output $\bar{F}^T$ to each of the two inputs depends on the frequency content of the input signal. The actuator behaves as a high-pass filter to length $\bar{L}^{MT}$ and as a low-pass filter to a(τ), with each having the same dimensionless cut-off frequency (i.e., $\tilde{\omega}_c = \tilde{k}^T$). Dimensionless angular frequency is defined as $\tilde{\omega} = \omega \cdot \tau_c = \omega \cdot (L_o^M/v_m)$.

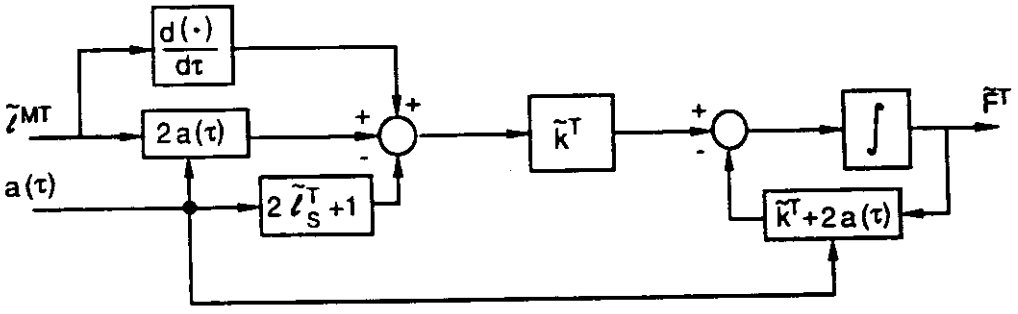


FIGURE 17. Block diagram of an actuator operating on the ascending region of the fl curve of its muscle fibers (case 2). Notice that a(τ) affects the forward gain to length $\tilde{L}^{MT}$, as well as the time constant for force development (through the effect of a(τ) on the feedback gain).

these muscles is mixed, their absolute cut-off frequencies are expected to be high (i.e., $\omega_c = \tilde{\omega}_c/0.1 > 300$ rad/s). In contrast, should any of these actuators have only slow muscle tissue, their cut-off frequencies would be 2 to 3 times lower.

Once the absolute cut-off frequency of an actuator is estimated, its ability to function as a spring or a dashpot during a motor task can be assessed. For example, hip actuators may well operate as dashpots during walking, since hip angular motion at normal gait speeds has a frequency content of less than 5 Hz (i.e., $\omega < \sim 30$ rad/s).[167,168] That is, actuator length $\tilde{L}^{MT}$ is expected to change relatively slowly because $\omega < \sim 30$ rad/s, which is less than the high-pass cut-off frequency $\omega_c$ for hip muscles (i.e., $\omega_c > 300$ rad/s). Also, because of their high cut-off frequencies, hip actuators will respond quickly to changes in activation. Since the lag from activation to force output will be negligible, the overall lag from neural input to force output is probably dominated by the lag from neural input to activation (i.e., by the lag caused by activation dynamics; see Section IV.E). Besides acting as *dashpots* during walking, hip actuators could also be considered to act as *velocity servos* with the velocity set-point of each actuator controlled by its activation (Figure 16A).

## F. MUSCULOTENDON CONTRACTION DYNAMICS WHEN MUSCLE OPERATES ON THE ASCENDING REGION OF ITS FL CURVE (CASE 2)

The dynamics is once again developed and analyzed and then employed, for illustrative purposes, to study the function of knee extensors during walking. To develop the dynamics of an actuator when its muscle fibers operate on the ascending region of their fl curve, recognize from Figure 15 that

$$-\tilde{v}^{M} = (2\,\tilde{L}^{M} - 1)\,a(\tau) - \tilde{F}^{M} \tag{19}$$

and with Equations 13 and 19 into Equation 15 the dynamics become (since $\tilde{F}^{T} = \tilde{F}^{M}$)

$$\frac{d\tilde{F}^{T}}{d\tau} + \left[\tilde{k}^{T} + 2a(\tau)\right] \cdot \tilde{F}^{T} = \tilde{k}^{T} \cdot \left\{\tilde{v}^{MT} + 2a(\tau)\,\tilde{L}^{MT} - (2\,\tilde{L}^{T}_{s} + 1)\,a(\tau)\right\} \tag{20}$$

A block diagram of the dynamics is shown in Figure 17. Notice that even when the characteristics of muscle and tendon are linearized, the nonlinearity of the dynamics is still evident, since a(τ) affects both the rate constant for force development, which is $[\tilde{k}^{T} + 2a(\tau)]$, and the responsiveness of an actuator to its length $\tilde{L}^{MT}$ (i.e., gain = 2 a(τ)). The rate constant is affected by a(τ) because the velocity-axis intercept of the fv curve (i.e., $v_m$) is assumed to be affected multiplicatively by a(τ) and $\tilde{L}^{M}$, and $\tilde{L}^{M}$ is in turn proportional to $\tilde{F}^{T}$ by the

amount of tendon compliance (i.e., $1/\tilde{k}^T$, see Equation 13). $a(\tau)$ affects the responsiveness of an actuator to its length $\tilde{L}^{MT}$ because $a(\tau)$ is assumed to affect the slope of the fl curve of the muscle fibers (e.g., Figure 5A and B).

A small-signal analysis can be performed to study how $a(\tau)$ and $\tilde{L}^{MT}$ affect force. Thus, let $a(\tau) \approx$ constant = A < 1 and $\tilde{L}^{MT} \approx$ constant = L. A block diagram and the frequency response of an actuator to $\tilde{L}^{MT}$ and $a(\tau)$ are shown in Figure 18, where $a(\tau)$, $\tilde{L}^{MT}$, and $\tilde{F}^T$ now refer to small perturbations about an operating point.

An actuator operates as a *spring* at low and high frequencies, and as a *dashpot* in between (i.e., as a dashpot when $2A < \tilde{\omega} < \tilde{k}^T + 2A$ (see Figure 18A). Thus, to changes in length $\tilde{L}^{MT}$, an actuator has "lead-lag" characteristics. An actuator behaves as a spring at low frequencies (i.e., $\tilde{\omega} < 2A$) because the fl relation of the muscle dominates the dynamics, and at high frequencies (i.e., $\tilde{\omega} > \tilde{k}^T + 2A$) because tendon compliance dominates. In contrast, an actuator operating on the flat region of the fl curve of the muscle acts as a spring only at high frequencies, when tendon compliance dominates (compare Figure 18A with Figure 16B [left plot]).

The *frequency band*, where an actuator behaves as a dashpot, depends not only on the one parameter $\tilde{L}_s^T$ of the actuator (since $\tilde{k}^T = 30/\tilde{L}_s^T$), but also on how much the actuator is activated (i.e., the activation level A (see Figure 18A). Notice that the width of the frequency band where the actuator acts as a dashpot ($\Delta\tilde{\omega} \equiv \tilde{\omega}_2 - \tilde{\omega}_1 = \tilde{k}^T$) is wider for stiff-tendon actuators (compare Figure 19A with Figure 19C). For stiff-tendon actuators at low activation, this frequency band can be 2 decades wide (see Figure 19A, dashed line). When either stiff- or compliant-tendon actuators are highly activated, the band shifts somewhat to higher frequencies, but, more importantly, the band narrows (compare dashed with solid lines in Figure 19A and C).

To neural input (i.e., activation), an actuator acts again as a low-pass filter (compare Figure 18B with Figure 16B [right plot]). However, when an actuator operates on the ascending region of its fl curve, it has a broader pass-band than when it operates on the flat region (compare $\tilde{\omega}_2 = \tilde{k}^T + 2A$ in Figure 18B with $\tilde{\omega}_c = \tilde{k}^T$ in Figure 16B [right plot]). As expected, a stiff-tendon actuator operating at any activation level has a more broad-band frequency response than a compliant-tendon actuator (compare Figure 19B with Figure 19D). Finally, the cut-off frequency of an actuator increases somewhat with activation, though its gain is compromised (compare dashed and solid lines in Figures 19B and D). The frequency response changes accompanying an increase in the average level of activation A are caused by more effective negative feedback (see Figure 18B, block diagram). Feedback gain increases because isometric muscle force, which is the variable driving the dynamics, fluctuates more to a given perturbation in length because the muscle fl curve is steeper when muscle activation is high.

Next I would like to use these dimensionless frequency response properties to show that the vastus lateralis (VL) during human walking probably functions as a dashpot (i.e., as an energy-dissipative element). In contrast to an actuator operating on the flat region of its fl curve, when only its $\tilde{L}_s^T$, $\tau_c$, and the frequency content of its motion are needed to determine its function, the average activation level A of an actuator must also be specified when it operates on the ascending region of its fl curve. First, the VL has a $\tilde{L}_s^T \approx 3$ (i.e., $\tilde{k}^T = 30/\tilde{L}_s^T = 10$) (see Table 1).[161] Second, since the VL is a mixed muscle, $\tau_c = 0.1$ s can be assumed. Third, for a nominal, natural walking cadence, and since the VL is active only during stance (about 50% of the stride), during which the knee first flexes and then extends,[168] the VL length $\tilde{L}^{MT}$ can be assumed to move at a frequency of ~2 Hz. Therefore, the VL operates at a frequency of $\omega \approx 13$ rad/s or, equivalently, $\tilde{\omega} = \omega \cdot \tau_c \approx 1.3$. Finally, the VL probably operates submaximally on the ascending region of its fl curve, since walking does not normally require maximum effort and the knee is near full extension during stance (i.e., the knee flexes 20° from full extension).[161,168] Therefore, a low activation level A can be

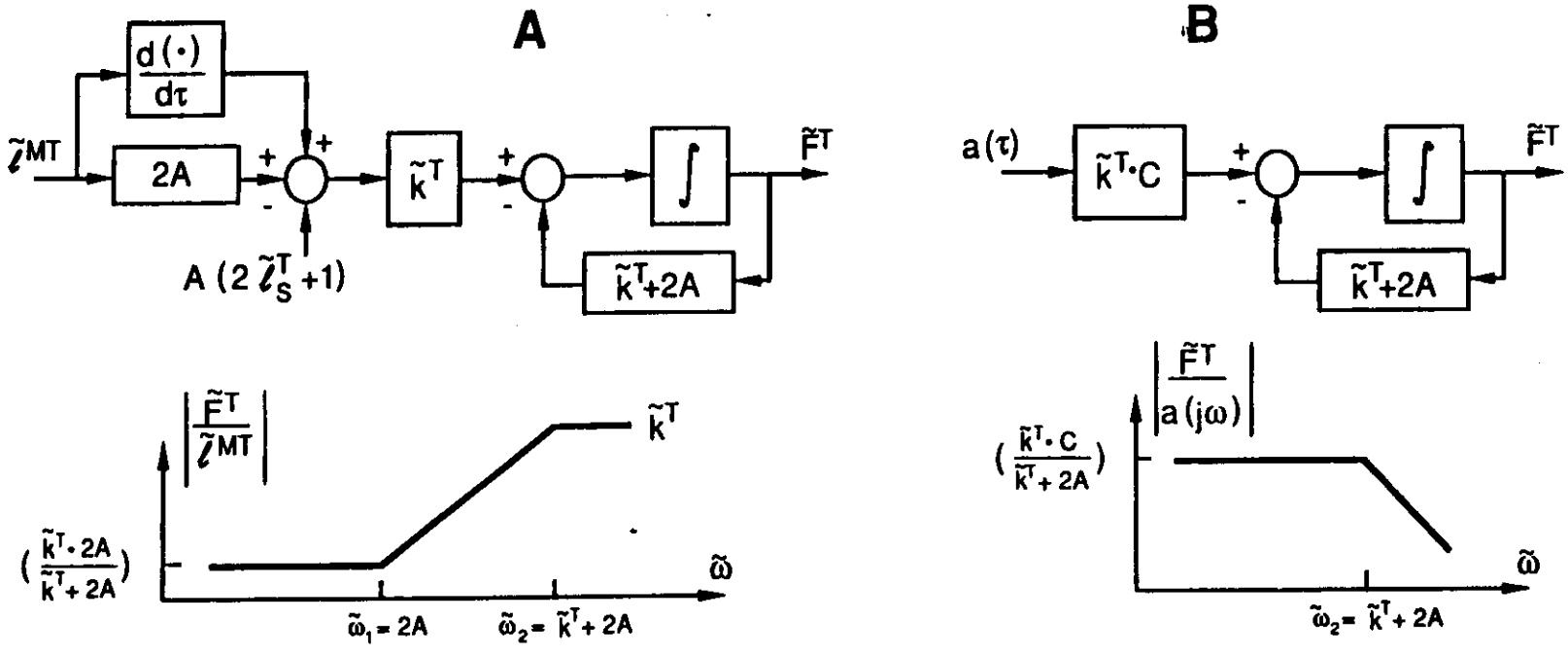


FIGURE 18. Block diagram and dimensionless frequency response of an actuator operating on the ascending region of the fl curve of its muscle fibers (case 2). The block diagrams are on top and the frequency response plots to length $\tilde{L}^{MT}$ (A) and activation a(τ) (B) are underneath. The actuator activation and length are assumed to fluctuate about an operating point, which is a(τ) = A and $\tilde{L}^{MT}$ = L. (A) The actuator has a lead-lag response to actuator length $\tilde{L}^{MT}$. Because of the flat response to both low and high frequencies, the actuator acts as a *spring* everywhere except in a band of frequencies ($2A < \tilde{\omega} < \tilde{k}^T + 2A$), where it functions as a *dashpot*. (B) The actuator acts as a low-pass filter to activation a(τ) with a cut-off frequency $\tilde{\omega}_2 = \tilde{k}^T + 2A$. Definition for "C" is $C \equiv 2\tilde{L}^{MT} - 2\tilde{L}_s^T - 1$.

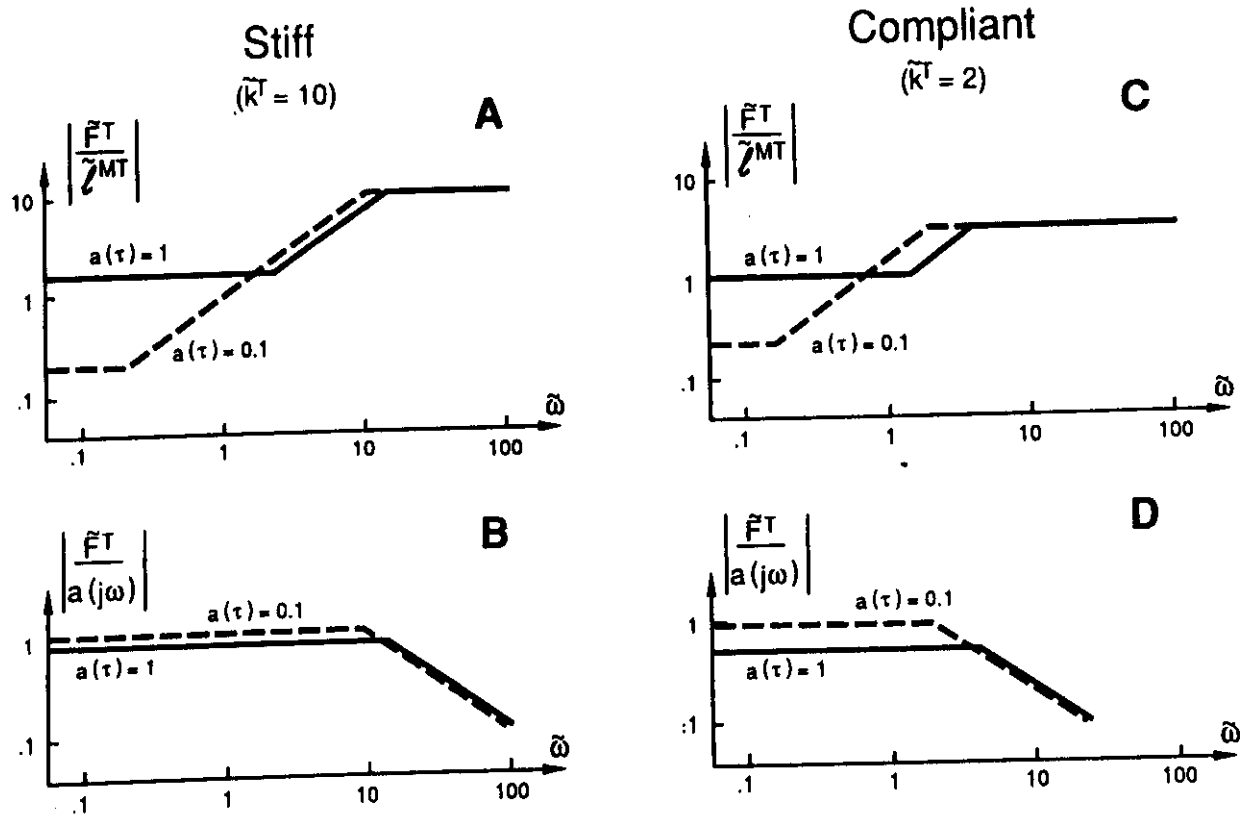


FIGURE 19. Dimensionless frequency response of a stiff tendon (A, B) and a compliant tendon (C, D) actuator when muscle activation is low ($a(\tau) = 0.1$; dashed lines) and high ($a(\tau) = 1.0$; solid lines). The actuators are assumed to be operating on the ascending region of their fl curves (case 2). Notice that the lead-lag response band to $\tilde{L}^{MT}$ is narrower at higher activations (A, C), but the actuator response to changes in activation is barely affected by the background activation level (B, D). Note that a stiff compared to a compliant actuator response to either $\tilde{L}^{MT}$ or $a(\tau)$ is more broad-band (compare A, B with C, D).

assumed (e.g., A = 0.1). Referring to Figure 19A (dashed line), and specifically to the point corresponding to $\tilde{\omega} \approx 1.3$, it follows that the VL acts within the band of frequencies where it is sensitive to velocity. Thus, the VL is expected to damp the motion of the knee.

However, if the VL should be much weaker than nominal, then it would not dampen knee motion as effectively because the frequency band where the VL would act as a dashpot would shrink (e.g., Figure 19A, compare $a(\tau) = 0.1$ with $a(\tau) = 1.0$). Also, if the VL should either be much slower, or have muscle fibers that are much shorter, or both, then it would operate at relatively higher frequencies (i.e., $\tilde{\omega}$ would be higher). Again, the ability of the VL to damp knee motion would be hindered. Since the effects of weak, slow, and short-fibered muscles compound, some individuals may have to walk at a lower cadence to achieve the desired damping effect from the VL.

## G. IS ACTIVATION OR MUSCULOTENDON-CONTRACTION DYNAMICS RATE-LIMITING?

To answer this question, the dimensionless time constant for buildup in activation from the neural input ( $\tilde{\tau}_{act}$ in Equation 5), which is associated with *activation dynamics* (see Figure 10B), will be compared with the dimensionless time constant for buildup in force from activation (called $\tilde{\tau}_{MT}$, see below), which is associated with *musculotendon contraction dynamics* (see Figure 10B). Should either of the two time constants be much larger than the other, then the overall dynamics of the actuator (see Figure 10B) will be rate-limited by the slowest dynamical process (i.e., the one with the longer time constant).

First, $\tilde{\tau}_{act}$ must be estimated. Based on data obtained from single fibers at 35°C,[119] $\tilde{\tau}_{act}$ can be calculated from the buildup in isometric tetanic tension, since isometric muscle fiber force corresponds to activation (see Section II.C). Thus, $\tilde{\tau}_{act} = 0.012$ s. The rise and fall of tetanic tension in isometric muscle depend on temperature, and when sensitivity to temperature is considered, the rise and fall of tension found in single fibers are similar to tension rise and fall in multifibered and whole-muscle rat and mouse preparations.[113,119,171,172] The time constant $\tilde{\tau}_{act} = 0.012$ s is, however, somewhat faster than that used by others to model human muscle.[16,79] I believe their estimates of $\tilde{\tau}_{act}$ are slower, because low temperatures were used in the "muscle" preparations from which many of their estimates are based. In addition, these experiments on isometric mammalian "muscles" are often, in reality, experiments on the isometric musculotendon actuator; thus the measured force (i.e., the tendon force) is affected by both musculotendon contraction dynamics and activation dynamics (e.g., see Figure 10B and C). That is, because of the inclusion of external tendon or muscle aponeurosis in the preparation, muscle fibers are not isometric even though the actuator is.

Assuming $\tau_c = 0.1$ s for fast muscle tissue, and activation in slow muscle tissue is a time-scaled version of fast-tissue dynamics (see Section II.D), then the dimensionless activation time-constant is from Equation 5:

$$\tilde{\tau}_{act} = 0.12 \tag{21}$$

Next, the dimensionless time constant for force buildup from activation ( $\tilde{\tau}_{MT}$) must be estimated. It is given by the reciprocal of the dimensionless, low-pass cut-off frequency (i.e., $1/\tilde{\omega}_c$ in Figure 16, and $1/\tilde{\omega}_2$ in Figure 18). Therefore,

$$\tilde{\tau}_{MT} \approx 1/\tilde{k}^T \approx \tilde{L}_s^T/30 \tag{22}$$

Thus the ratio of musculotendon time constant to activation time constant is

$$\frac{\tilde{\tau}_{MT}}{\tilde{\tau}_{act}} \approx 0.3\,\tilde{L}_s^T \tag{23}$$

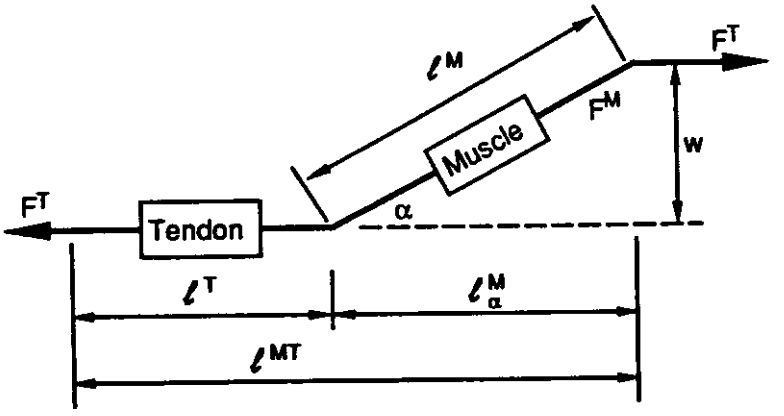


FIGURE 20. Schema to show the relation among muscle fiber length $L^M$ and force $F^M$, tendon length $L^T$ and force $F^T$, and musculotendon length $L^{MT}$. Notice that the contribution of muscle to musculotendon length (i.e., $L^M_\alpha$) depends on the pennation angle α (i.e., $L^M_\alpha = L^M \cos \alpha$).

To assess whether musculotendon-contraction or activation dynamics limits the responsiveness of force to neural excitation in a specific actuator, its one dimensionless parameter $\tilde{L}^T_s$ must be substituted into Equation 23. For example, human actuators with very long tendons (e.g., the soleus with $\tilde{L}^T_s = 11$), moderately long tendons (e.g., the rectus femoris with $\tilde{L}^T_s = 5$), and short tendons (e.g., uniarticular hip muscles with $\tilde{L}^T_s < 1$) (see Table 1) have ratios of:

$$\begin{aligned} &\tilde{\tau}_{MT}/\tilde{\tau}_{act} = 3.3 \quad \text{soleus} \\ &\tilde{\tau}_{MT}/\tilde{\tau}_{act} = 1.5 \quad \text{rectus femoris} \\ &\tilde{\tau}_{MT}/\tilde{\tau}_{act} < 0.3 \quad \text{uniarticular hip muscles} \end{aligned} \tag{24}$$

Thus, with respect to force generation, musculotendon dynamics is the rate-limiting process in the soleus, activation dynamics in uniarticular hip muscles, and both dynamics significantly affect force generation in the rectus femoris. The suggestion that musculotendon dynamics, which are set by tendon compliance, are rate-limiting to soleus force development and, in general, to the force development of any long-tendon actuator, is consistent with others' views that tendon compliance impacts critically on the overall functioning of muscles (i.e., actuators) residing distally in the upper and lower extremities of mammals, including humans.[5,9,34,37-39,41,91,154]

## H. MUSCLE FIBER PENNATION

In this section, relations are developed to show that muscle fiber pennation must be very high to affect the static and dynamic properties of actuators. Figure 20 shows the relation between tendon and muscle force, and the relations among musculotendon, muscle fiber, and tendon length, i.e.,

$$\begin{aligned} F^T &= F^M \cos \alpha \\ L^{MT} &= L^T + L^M_\alpha;\ L^M_\alpha \equiv L^M \cos \alpha \end{aligned} \tag{25}$$

If the distance between the aponeurosis of origin of the muscle and insertion remains con-

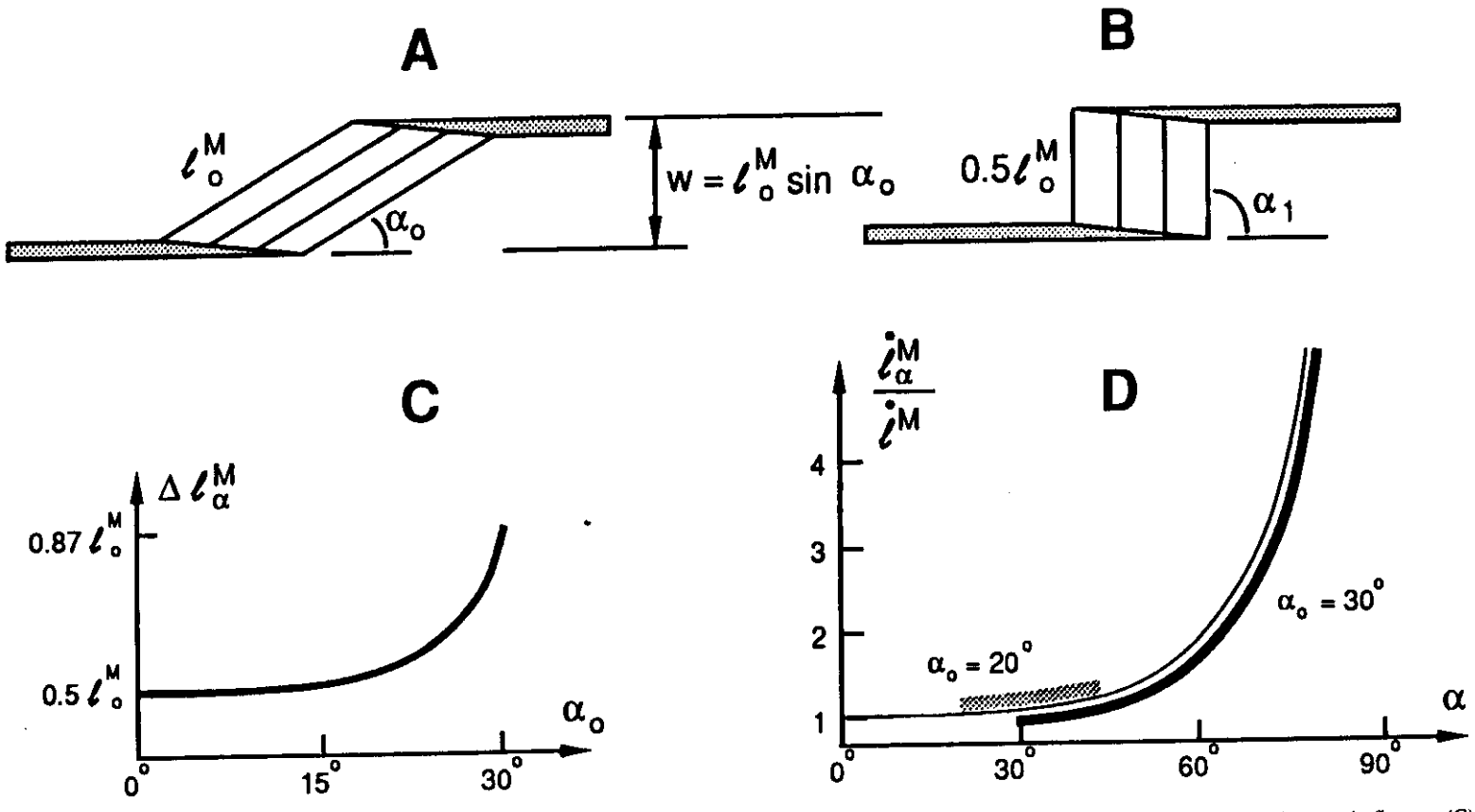


FIGURE 21. Effects of pennation on musculotendon velocity (D) and the range of musculotendon lengths corresponding to the ascending region of the muscle fl curve (C). Tendon is assumed to be compliantless so that the effects of pennation alone can be analyzed. Muscle thickness $w$ is assumed to be constant, causing pennation to increase as fibers shorten. (A, B) Geometry of muscle fibers with respect to tendon when fibers are at their optimal length $L_o^M$, corresponding to a pennation angle of $\alpha = \alpha_o$ (e.g., $\alpha_o = 30°$ in A), and when fibers are at their shortest length $L^M = 0.5L_o^M$, corresponding to an $\alpha = \alpha_1$ (e.g., $\alpha_1 = 90°$ in B). (C) Decrease in musculotendon length $\Delta l_\alpha^{MT}$ as fibers shorten from $L_o^M$ to $0.5L_o^M$. Notice that an actuator must shorten further than its muscle fibers (i.e., $\Delta l_\alpha^{MT} > 0.5L_o^M$), especially when fibers are highly pennated ($\alpha_o = 30°$). (D) Musculotendon velocity $\dot{L}_\alpha^M$ is greater than muscle fiber velocity $\dot{L}^M$, especially if fibers enter into a region of high pennation. This region can be reached only in actuators having highly

stant (w, see Figure 21A and B).[41-45] then fibers contribute less to musculotendon length ($L_\alpha^M$) as they shorten and become more pennated. In addition, with pennation, tendon force $F^T$ is less than muscle force $F^M$.

The more pennated muscle fibers are the larger the change in musculotendon length caused by a change in the fiber length. To show this assume that muscle fibers can shorten up to one half their optimal length $L_o^M$. Let $\alpha_o$ be the pennation angle corresponding to $L_o^M$ (see Figure 21A). Then, $\alpha_o \leq 30°$ because, when $\alpha_o = 30°$, fully shortened muscle fibers will be perpendicular to the tendon (i.e., $\alpha_1 = 90°$ when $L^M = 0.5L_o^M$, see Figure 21B).[42] In this case, the decrease in musculotendon length $\Delta L_\alpha^M$ caused by fibers shortening from $L_\alpha^M$ to $0.5L_o^M$ is

$$\Delta L_\alpha^M = L_o^M \cos \alpha_o - 0.5L_o^M \cos \alpha_1 = 0.87L_o^M;\ \alpha_o = 30 \tag{26}$$

Thus, a $0.5L_o^M$ decrease in muscle fiber length in an actuator, which has an initial muscle-fiber pennation of 30°, causes a $0.87L_o^M$ decrease in musculotendon length $\Delta L_\alpha^M$.

However, in most actuators, except in those having highly pennated muscles (e.g., $\alpha_o \approx 30°$), the change in musculotendon length $\Delta L_\alpha^M$ mimics the $0.5L_o^M$ change in fiber length (see Figure 21C). Specifically, notice that the change in musculotendon length occurring in actuators with little pennation ($\alpha_o < 20°$) is about equal to the change occurring in actuators with zero pennation (i.e., for $\alpha_o = 0$, $\Delta L_\alpha^M = L_o^M - 0.5L_o^M = 0.5L_o^M$).

The fact that the change in musculotendon length for a given change in muscle fiber length is greater in actuators having pennation implies that the rate of change of musculotendon length is greater than the rate of change of muscle fiber length (i.e., $\dot{L}_\alpha^M > \dot{L}^M$). In fact, $\dot{L}_\alpha^M = \dot{L}^M/\cos \alpha$.[42] Thus, the shorter the muscle fibers are relative to $L_o^M$, and therefore the more pennated they are relative to $\alpha_o$, the faster the actuator shortens per unit velocity of muscle fiber shortening. Figure 21D shows how pennation angle affects $\dot{L}_\alpha^M$ and, specifically for $\alpha_o = 20$ and 30°, the effect as fibers shorten from $L_o^M$ to their most contracted length. Notice that only in actuators with highly pennated muscles (i.e., $\alpha_o$ near 30°) will actuator velocity $\dot{L}_\alpha^M$ deviate significantly from muscle fiber velocity.

To conclude, the effects of pennation on musculotendon properties are significant only when muscle fibers are highly pennated. In the human lower extremity, for example, significant effects would be expected in only the soleus and the short-head of the biceps femoris, which have $\alpha_o = 25°$ and 23°, respectively.[122]

## I. MECHANICAL ENERGETICS OF TENDON AND MUSCLE

Storage of elastic energy in the musculotendon actuator for subsequent release is often hypothesized to be a mechanism used by man and animals to efficiently locomote or perform other motor tasks.[5,9,33-40,138,140-142] Based on the material properties of muscle and tendon given in previous sections, the ratio of elastic energy in tendon to muscle will be shown to be proportional to both the force in the actuator and the ratio of tendon slack length to muscle fiber length $\tilde{L}_s^T$. Though tendon elastic energy is shown to either dominate or contribute significantly to the total elastic energy of an actuator, it is concluded that models must be used to compute whether or not elastic energy plays an important role in the functioning of an actuator during a specific task. Thus, I will mention how actuator models can be used to compute total power and energy released from muscle and tendon during a motor task.

### 1. Elastic Energy Storage in Muscle and Tendon

To assess the relative amount of elastic energy stored in tendon to muscle requires that not only the elasticity of tendon be accounted for, which indeed has been done throughout this review, but also the elasticity of muscle. However, muscle SEE, which is indeed the elastic element that must be proposed to account for the active stiffness of muscle has been assumed to be nonexistent. (Any energy stored in the PEE is excluded from consideration in

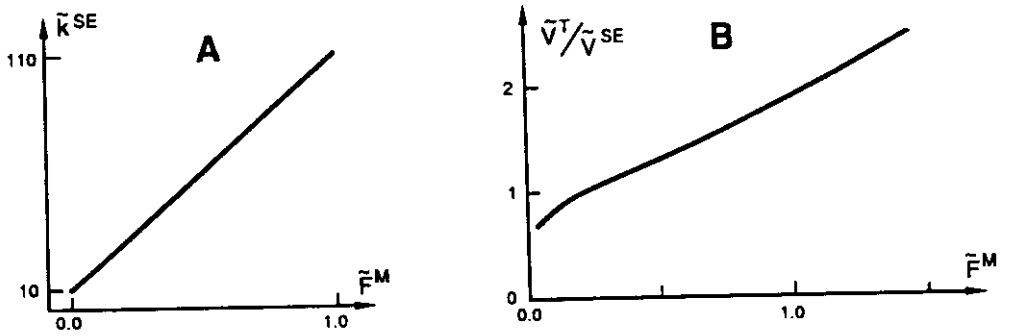


FIGURE 22. Dimensionless stiffness of muscle (A) and the ratio of dimensionless elastic energy storage in tendon to muscle (B). (A) Dimensionless stiffness of muscle ($\tilde{k}^{SE} = k^{SE} \cdot [L_o^M/F_o^M]$) is assumed to increase linearly with muscle force $\tilde{F}^M$, concomitant with the increase in the number of cross-bridges in muscle. From this curve, the dimensionless elastic energy of muscle $\tilde{V}^{SE}$ at any force $\tilde{F}^M$ can be calculated (see text). (B) Notice that the dimensionless elastic energy of tendon (calculated from Figure 9B) relative to muscle (i.e., $\tilde{V}^T/\tilde{V}^{SE}$) increases about linearly with force $\tilde{F}^M$. $\tilde{F}^M = \tilde{F}^T$ is assumed.

this discussion.) One reason for excluding muscle SEE (see Section II.B) is that in all but short tendon actuators, little elastic energy is stored in muscle, as follows.

Assume that the *muscle stiffness* resides in the cross-bridges and that the energy stored in these cross-bridges is purely elastic and therefore recoverable. Commonly, muscle stiffness is assumed to increase with active muscle force (see Figure 22A). This relation is based on values found for the stiffness of single muscle fibers and the ("short-range") stiffness of "whole" muscle, is more or less a lower limit to the stiffness associated with the elasticity residing in the cross-bridges, and is compatible with a fall in muscle fiber force from $F_o^M$ to zero during controlled instantaneous releases of $1.1\%L_o^M$.[24,25,36,37,49,50,87-89,91-92,153,169,170]

The *dimensionless elastic energy stored in active muscle* $\tilde{V}^{SE}$ at a given force $\tilde{F}^{CE} = \tilde{F}^M$ (since $\tilde{F}^{PE} = 0$, by assumption) can be calculated from the stiffness-force relationship (the $\tilde{k}^{SE}$ vs. $\tilde{F}^M$ curve) shown in Figure 22A, i.e.,

$$\tilde{V}^{SE} = \int \left( \frac{\tilde{F}^M}{\tilde{k}^{SE}} \right) d\tilde{F}^M \tag{27}$$

Notice that the elastic energy of muscle is a function of $\tilde{F}^M$ or, equivalently, $\tilde{F}^T$ (since $\tilde{F}^T = \tilde{F}^M$). The *dimensionless elastic energy stored in tendon* $\tilde{V}^T$ is the area under its $\tilde{F}^T$ vs. $\Delta\tilde{L}^T$ curve (obtainable from Figure 9B by recognizing that $\Delta\tilde{L}^T = \varepsilon^T \cdot \tilde{L}_s^T$), and also depends on $\tilde{F}^T$.

The ratio of *dimensionless* elastic energy stored in tendon to muscle $\tilde{V}^T/\tilde{V}^{SE}$ thus depends on the dimensionless force in tendon $\tilde{F}^T$. This ratio varies about linearly with $\tilde{F}^T$ over a wide range of $\tilde{F}^T$ (see Figure 22B). The reason the ratio increases with $\tilde{F}^T$ is that muscle stiffness rises with force more steeply than tendon stiffness. Thus,

$$1 < \left( \frac{\tilde{V}^T}{\tilde{V}^{SE}} \right) < 2.5; \; 0.1 < \tilde{F}^T < 1.5 \tag{28}$$

Bounds on the ratio of the *absolute* elastic energy stored in the tendon to the *absolute* elastic energy stored in the muscle $V^T/V^{SE}$ of a specific actuator can now be found as a function of its one dimensionless parameter $\tilde{L}_s^T$. First, the *absolute elastic energy in tendon* $V^T$ and the *absolute elastic energy in muscle* $V^{SE}$ are related to their dimensionless energies:

$$V^T = \tilde{V}^T \cdot F_o^M \cdot L_s^T \text{ and } V^{SE} = \tilde{V}^{SE} \cdot F_o^M \cdot L_o^M \tag{29}$$

Next recall that $\tilde{L}_s^T \equiv L_s^T/L_o^M$. Therefore, from Equations 28 and 29

$$\frac{V^T}{V^{SE}} = \left(\frac{\tilde{V}^T}{\tilde{V}^{SE}}\right) \cdot \tilde{L}_s^T \tag{30}$$

Since $\tilde{V}^T/\tilde{V}^{SE}$ is bounded (see Equation 28), the ratio of absolute elastic energies $V^T/V^{SE}$ is also bounded and given by

$$1 < \left(\frac{V^T}{V^{SE}}\right) \cdot \frac{1}{\tilde{L}_s^T} < 2.5;\ 0.1 < \tilde{F}^T = F^T/F_o^M < 1.5 \tag{31}$$

It follows from Equation 31 that elastic energy storage in long tendon actuators (e.g., $\tilde{L}_s^T = 10$) resides in tendon and not in muscle. Even for extremely stiff actuators (i.e., $\tilde{L}_s^T = 0.1$), the contribution of the tendon to elastic energy storage is 10 to 25% that of muscle. Given that the storage of energy in cross-bridges is controversial in the sense of being elastically recoverable[49,88] and that many actuators have $\tilde{L}_s^T > 1$ (see Table 1), only for very stiff tendon actuators will muscle stiffness be a dominant site for storage of elastic energy.[34]

## 2. Power and Energy Released by Muscle and Tendon

Given that tendon is the dominant site for elastic energy storage in all but very short-tendon actuators, the next question is how important is the release of elastic energy in tendon to the energy output from the muscle fibers? Unfortunately, computer simulations are needed to answer this question, since energy output is path-dependent.

The reason the question cannot be answered is that an upper bound on the ratio of net energy output from tendon to muscle is unspecifiable. However, a lower bound can be set. First, assume that tendon releases during shortening 93% of the energy it has stored.[138,142] Second, assume that muscle always generates maximum force (i.e., force is set by the its fl relation, and reduction in force due to its fv property is neglected). Even though the following assumption increases somewhat the lower-bound estimate, assume that any force enhancement in muscle fibers during shortening subsequent to their prestretching, if any, is negligible.

A lower bound on the ratio of net energy output from tendon to muscle is then given by the ratio of the areas under their fl curves. Defining $E^T$ as the *energy output from tendon* and $E^M$ as the *energy output from muscle*, I can show from Figures 8A and 9B that when force is high the lower bound becomes approximately:

$$\frac{E^T}{E^M} > 0.07 \cdot \tilde{L}_s^T \cdot a(t);\ 0 < a(t) < 1 \tag{32}$$

The reason the ratio decreases with a decrease in a(t) is because muscle fibers must be held at a longer length to bear a given force when submaximally activated, causing the area under its fl curve to be higher (e.g., refer to Figures 5A and B and calculate areas when $F^M = F_o^M$).

An upper bound on the ratio of net energy output from tendon to muscle $E^T/E^M$ is unspecifiable because a lower bound on muscle energy output $E^M$ cannot be estimated confidently. For example, when muscle undergoes a fast shortening, some of its energy is lost due to its fv property. Thus energy output from muscle will be less than the area under its fl curve, but how much less? Unfortunately, a computer simulation based on a model of muscle must be performed to calculate how much energy is lost.

Using models of muscle and tendon, the net mechanical power and energy output from tendon and muscle can be computed:

$$\text{tendon:} \quad \text{power output} = -(F^T \cdot v^T) \qquad \text{energy output} = -\int (F^T \cdot v^T)dt$$

$$\text{muscle:} \quad \text{power output} = -(F^M \cdot v^M) \qquad \text{energy output} = -\int (F^M \cdot v^M)dt \tag{33}$$

Of course, power and energy absorbed by tendon and muscle are just opposite in sign. Since power is state-dependent (i.e., both force- and velocity-dependent) and energy is state-trajectory dependent, mechanical models of musculotendon actuators, for example, as presented here, must be formulated and Equation 33 used to calculate net power and energy output from muscle and tendon.

For example, to estimate muscle and tendon power and energy, recordings of the EMG signal and the length and velocity of the musculotendon actuator during the motor task can be made. These three trajectories can be considered to act as inputs to a musculotendon actuator model (e.g., see Figures 10 and 14) from which tendon and muscle force can be computer estimated. Equation 33 can then be used to estimate the mechanical energetics or power associated with the motor task. Indeed, such models have been used to study the function of human calf muscles during walking and jumping.[5,9]

Summarizing this and the preceding section, tendon will often be the dominant site of elastic energy storage, but elastic energy storage in tendon may not dominate the energy output of an actuator. Energy output from muscle, and not necessarily from its elastic structures, may instead dominate. To ascertain the individual contribution of tendon and muscle to actuator energy output, computer simulations must be employed.

## J. COMPUTER IMPLEMENTATION OF MUSCULOTENDON ACTUATOR MODELS

Clearly, there is a trade-off between the complexity of a model and the computational and intellectual time associated with its implementation. More complex models for muscle than those discussed here, which are based on cross-bridge mechanisms, have been developed.[24] These more complex models have not, however, been used in computer simulations that demand the modeling of many muscles, such as in studies of body-segmental coordination. The reason is that these more complex representations of muscle function are specified by partial differential equations involving quantities that are far removed from the net mechanical function of the muscle. Thus, not only would computation time be greatly increased compared with the time to solve the first-order ordinary differential equations presented here, but parameter identification would be formidable because much less is known about how these microquantities vary among species and muscles than how macroquantities do.

The musculotendon contraction dynamics expressed in Equation 16 assume that the flv relationship is invertible, i.e., given that force $F^M = f(L^M, v^M, a(t))$, we can find $v^M = f^{-1}(F^M, L^M, a(t))$. Such invertibility may not always be possible because $F^M$ may not be a single-valued function of $v^M$. Even if the relation is single valued (e.g., see Figure 5C), computational problems can arise if the velocity intercept is assumed to be constant for all $a(t)$ and $L^M$. The problem arises because when velocity is computed by taking the inverse, division by a very small number occurs. The small number appears because the magnitude of the slope of the fv curve is small when isometric muscle force is small (e.g., when $a(t) << 1$ or $L^M << L_o^M$). We have resolved this computational problem by constraining $a(t)$ (i.e., $0 < a_{min} \leq a(t) \leq 1$).

A more satisfying way to solve the problem of invertibility is to recognize the root of the problem, which is the assumption that the acceleration of the mass of muscle does not influence the ability of muscle to generate force.[7a] All computer simulations of coordination to date embed muscle mass into the body-segmental mass that appears in the dynamical equations-of-motion of the body segments. In reality, the acceleration of the muscle mass relative to the acceleration of the body segments also needs to be considered. If this property

should be modeled, musculotendon contraction dynamics would then be second-order rather than first-order, and the state variables would be $L^M$ and $v^M$, rather than $F^T$. Even though the number of state variables would increase from one to two, such a formulation may actually cause computation time to decrease because of the otherwise high overhead of calculating muscle fiber velocity at low a(t) and small $L^M$.

In many optimization studies, all functions need to be at least twice-differentiable. Thus, for example, even if the fv relation of muscle is believed to be discontinuous in the first derivative at $v^M = 0$,[24,25] such discontinuities must often be smoothed for computer implementation. Nevertheless, through computer simulation, the impact of these approximations on the motor task can be assessed.

## V. CONCLUDING REMARKS

This review has focused on the modeling of the static and dynamic properties of tendon and muscle for use in computer simulations of muscle and body-segmental coordination. In addition, this review synthesized these properties and models to formulate a generic, dimensionless model of the musculotendon actuator. The model can be used to study the basic mechanical interactions between tendon and muscle and can also be scaled to assess the role of individual actuators during specific motor tasks.

Though such musculotendon models are meaningful to studies in which knowledge of net mechanical energy transfer among tendon, muscle, and body segments during movement is desired, these models per se do not specify the relationship between metabolic energy consumption and muscle-state variables.[49] Muscle models based on cross-bridge mechanics have potential in coupling the metabolic energetics to the mechanical events, but a very high computational price has to be paid.

A compromise that must be considered in future simulations, especially since computer performance per dollar invested continually rises, is the distribution-moment model derived from cross-bridge theories of muscular contraction.[96,173,174] This model is attractive because (1) it is only fourth-order, where the state variables are muscle fiber length, muscle force, stiffness, and elastic energy stored in the cross-bridges, (2) consumption of metabolic energy can be estimated, and (3) it can be coupled (or uncoupled) to a first-order model of activation dynamics.[96,97] For now, I believe that it is still too computationally intensive to be practical to simulations involving many muscles, though its use should be encouraged in simulations where emphasis is placed on how one or a few muscles function during movement.

The first-order model of musculotendon contraction dynamics discussed in this review can be considered an asymptotic (steady-state) approximation to the cross-bridge models.[24,50] Therefore, the simpler model may indeed suffice as a representation of the dynamical properties of musculotendon actuators as long as muscle force and length change "slowly". In studies of body-segmental coordination, I believe that joint angles and angular velocities do indeed change slowly relative to the changes that they would have to exhibit for muscle fibers to show nonsteady-state phenomena (e.g., "yielding" and "giving").[81,175,176] For example, experiments that show yielding, which occurs after the effects of muscle (cross-bridge) stiffness have subsided, often impose instantaneous changes in position or velocity on the muscle fibers. Such changes do not occur during natural, unperturbed movements, but indeed may occur when limbs are subjected to unexpected perturbations.

Also, in long tendon actuators, muscle fiber variables will change slowly, since tendons will change their length fast to absorb any quick change in musculotendon length. For example, consider heel strike during gait. Since long tendon actuators reside in the shank and foot (see Table 1), distal tendons may indeed absorb the "shock" at heel strike. Thus, length changes of muscle tissue in these actuators will be slower than the changes the actuator experiences. Muscle tissue in short tendon actuators, which reside more proximally, will,

however, experience the same length changes as their actuators. However, the lengths of these actuator are not expected to change fast because the inertial load of the body proximally is large. Therefore, all muscle tissue in limbs may operate "slowly" during natural, unperturbed movements.

Recent studies of muscle architecture indicate that the length of muscle fibers may be less than the length of the muscle fascicles in which they reside.[47,48] The basic structure of the model discussed in this review would still be applicable if $L^M$ were to represent "true" muscle fiber length rather than muscle fascicular length. Also, a SEE to represent the effective intramuscular elasticity of the *passive* intrafascicular filaments may have to be invoked. However, in this case its meaning would be quite distinct from its current one, which is that it represents *active* muscle stiffness. The total series compliance of passive structures (external- and internal-tendon compliance, plus intrafascicular-filament compliance) would obviously be greater than tendon compliance alone. Thus $\tilde{L}_s^T$, which would now correspond to the ratio of the slack length of the *combined passive structures* to the optimal length of the "true" muscle fibers, would even be higher than suggested in this review (e.g., higher than those in Table 1). If so, "tendon", as referred to in this review, which would now represent these "combined passive structures", would affect the musculotendon contraction dynamics and the function of the actuator even more.

This review did not include the role that local feedback (e.g., muscle length, velocity, and force) can have on the net input (neural)-output (force) properties of muscle.[177] Indeed, at times local feedback may act in concert with the properties of the musculotendon actuator to linearize the overall I/O response of muscle. Given that these feedback loops are probably gain-controlled by higher CNS structures, my preference is to include such feedback explicitly in models, when appropriate.

The evolution of models depends on the outcome of the comparison of modeling data with experimental data. Indeed, it is through such comparisons that we gain knowledge of the mechanisms responsible for the behavior under study. Once our models are compatible with the qualitative properties of the behavior, we can perform sensitivity studies to determine the parameters to which the behavior is most sensitive. These data then guide experiments into directions that must be pursued if relevant information is to be gathered to better comprehend the behavior. The use of computer models in conjunction with experiments is probably the only viable approach available to study complex, coordinated movements, just as it has been the only reasonable approach to the design of complex control systems for robots and spacecraft (i.e., we cannot just "wing" it).

## ACKNOWLEDGMENTS

This review was supported by NIH grant NS 17662 and the Veterans Administration. I thank W. S. Levine for the many discussions he and I have had on musculotendon modeling, and especially on computer implementation of these models. I thank Eric Topp, Pamela Stevenson, and Gon Khang for their contributions to the development, computer implementation, and computer simulation of a musculotendon model from which I gained much insight into the issues discussed in this review. I thank Melissa Hoy, Michael Gordon, Scott Delp, William Levine, Marcus Pandy, and Gon Khang for their many comments on an earlier version of the manuscript. I also thank David Delp for preparing the figures and Kristin Bennett for typing assistance.

## LIST OF SYMBOLS

$F^M$, $(\tilde{F}^M)$ = muscle force

$F^{CE}$, $(\tilde{F}^{CE})$ = contractile element force

$F^{PE}$, $(\tilde{F}^{PE})$ = passive element force
$F^{T}$, $(\tilde{F}^{T})$ = tendon force
$L^{S}$ = sarcomere length
$L^{M}$, $(\tilde{L}^{M})$ = muscle fiber length
$L^{T}$, $(\tilde{L}^{T})$ = tendon length
$L^{MT}$, $(\tilde{L}^{MT})$ = musculotendon, or actuator, length
$v^{M}$, $(\tilde{v}^{M})$ = muscle fiber velocity
$v^{T}$, $(\tilde{v}^{T})$ = tendon velocity
$v^{MT}$, $(\tilde{v}^{MT})$ = musculotendon, or actuator, velocity
$E^{M}$ = mechanical energy output from muscle
$E^{T}$ = energy output from tendon
$V^{SE}$, $(\tilde{V}^{SE})$ = elastic energy stored in muscle cross-bridges
$V^{T}$, $(\tilde{V}^{T})$ = elastic energy stored in tendon
$\omega$, $(\tilde{\omega})$ = angular frequency
$t$, $(\tau)$ = time
$\sigma^{T}$, $(\tilde{\sigma}^{T})$ = tendon stress
$\varepsilon^{T}$ = tendon strain
$u(t)$, $(u(\tau))$ = muscle excitation
$a(t)$, $(a(\tau))$ = muscle activation, or active state
$\alpha$ = muscle fiber pennation
$L_{\alpha}^{M}$ = length of muscle fibers having pennation $\alpha$, projected onto tendon axis of pull
$F_{o}^{M}$ = peak isometric active muscle force
$L_{o}^{M}$ = optimal muscle fiber length (i.e., length where peak active force is developed)
$\alpha_{o}$ = optimal muscle-fiber pennation angle (i.e., pennation angle $\alpha$ when $L^{M} = L_{o}^{M}$)
$\varepsilon_{o}^{T}$ = tendon strain when $F^{T} = F_{o}^{M}$
$\alpha_{o}^{M}$ = tendon stress when $F^{T} = F_{o}^{M}$
$L_{s}^{T}$, $(\tilde{L}_{s}^{T})$ = tendon slack length (ratio of tendon slack length to $L_{o}^{M}$)
$k^{SE}$, $(\tilde{k}^{SE})$ = stiffness of muscle cross-bridges
$k^{T}$, $(\tilde{k}^{T})$ = tendon stiffness
$v_{m}$ = maximum shortening velocity of muscle fibers
$\tau_{c}$ = time-scaling parameter (i.e., $\tau_{c} \equiv L_{o}^{M}/v_{m}$)
$\tau_{act}$, $(\tilde{\tau}_{act})$ = time constant for rise in muscle activation
$\tau_{deact}$, $(\tilde{\tau}_{deact})$ = time constant for fall in muscle activation
$\tau_{MT}$, $(\tilde{\tau}_{MT})$ = time constant of the musculotendon contraction process
$\omega_{c}$, $(\tilde{\omega}_{c})$ = cut-off angular frequency of the musculotendon contraction process

The symbols in parentheses represent the dimensionless form of the preceding physical variable or parameter, obtained by using $F_{o}^{M}$, $L_{o}^{M}$, and $\tau_{c}$ to scale the fundamental physical quantities of force, length, and time.

# REFERENCES


1. **Olney, S. J. and Winter, D. A.,** Prediction of knee and ankle moments of force in walking from EMG and kinematic data, *J. Biomech.*, 18, 9, 1985.
2. **Pierrynowski, M. R. and Morrison, J. B.,** Estimating the muscle forces generated in the human lower extremity when walking: a physiological solution, *Math. Biosci.*, 75, 43, 1985.
3. **Pierrynowski, M. R. and Morrison, J. B.,** A physiological model for the evaluation of muscular forces in human locomotion: theoretical aspects, *Math. Biosci.*, 75, 69, 1985.
4. **Pedotti, A., Krishnan, V. V., and Stark, L.,** Optimization of muscle-force sequencing in human locomotion, *Math. Biosci.*, 38, 57, 1978.
5. **Hof, A. L., Geelen, B. A., and Van den Berg, J. W.,** Calf muscle moment, work and efficiency in level walking; role of series elasticity, *J. Biomech.*, 16, 523, 1983.
6. **Zajac, F. E., Wicke, R. W., and Levine, W. S.,** Dependence of jumping performance on muscle properties when humans use only calf muscles for propulsion, *J. Biomech.*, 17, 513, 1984.
7. **Levine, W. S., Zajac, F. E., Belzer, M. R., and Zomlefer, M. R.,** Ankle controls that produce a maximal vertical jump when other joints are locked, *IEEE Trans. Autom. Control*, AC-28, 1008, 1983.

7a. **Levine, W. S.,** personal communication.

8. **Bobbert, M. F., Huijing, P. A., and van Ingen Schenau, G. J.,** A model of the human triceps surae muscle-tendon complex applied to jumping, *J. Biomech.*, 19, 887, 1986.
9. **Bobbert, M. F., Huijing, P. A., and van Ingen Schenau, G. J.,** An estimation of power output and work done by the human triceps surae muscle-tendon complex in jumping, *J. Biomech.*, 19, 899, 1986.
10. **Hatze, H.,** A comprehensive model for human motion simulation and its application to the take-off phase of the long jump, *J. Biomech.*, 14, 135, 1981.
11. **Hatze, H.,** The complete optimization of a human motion, *Math. Biosci.*, 28, 99, 1976.
12. **Clark, M. R. and Stark, L.,** Control of human eye movements. I. Modelling of extraocular muscle, *Math. Biosci.*, 20, 191, 1974.
13. **Clark, M. R. and Stark, L.,** Control of human eye movements. II. A model for the extraocular plant mechanism, *Math. Biosci.*, 20, 213, 1974.
14. **Clark, M. R. and Stark, L.,** Control of human eye movements. III. Dynamic characteristics of the eye tracking mechanism, *Math. Biosci.*, 20, 239, 1974.
15. **Bahill, A. T., Latimer, J. R., and Troost, B. T.,** Linear Homeomorphic model for human movement, *IEEE Trans. Biomed. Eng.*, 27, 631, 1980.
16. **Winters, J. M. and Stark, L.,** Analysis of fundamental human movement patterns through the use of in-depth antagonistic muscle models, *IEEE Trans. Biomed. Eng.*, BME-32, 826, 1985.
17. **Gottlieb, G. L. and Agarwal, G. C.,** Dynamic relationship between isometric muscle tension and the electromyogram in man, *J. Appl. Physiol.*, 30, 345, 1971.
18. **Herzog, H.,** Individual Muscle Force Prediction in Athletic Movements, Ph.D. thesis, University of Iowa, Iowa City, 1985.
19. **Winters, J. M. and Stark, L.,** Muscle models: what is gained and what is lost by varying model complexity, *Biol. Cybern.*, 55, 403, 1987.
20. **Perry, J. and Bekey, G. A.,** EMG-force relationships in skeletal muscle, *CRC Crit. Rev. Bioeng.*, 7, 1, 1981.
21. **Audu, M. L. and Davy, D. T.,** The influence of muscle model complexity in musculoskeletal motion modeling, *J. Biomech. Eng.*, 107, 147, 1985.
22. **Hatze, H.,** A myocybernetic control model of skeletal muscle, *Biol. Cybern.*, 25, 103, 1977.
23. **Partridge, L. D. and Benton, L. A.,** Muscle, the motor, in *Handbook of Physiology. The Nervous System*, Section 1, Vol. 2 (Part 1), American Physiological Society, Bethesda, MD, 1981, chap. 3.
24. **Huxley, A. F.,** A hypothesis for the mechanism of contraction, *Prog. Biophys. Biophys. Chem.*, 255, 1957.
25. **Huxley, A. F.,** Review lecture: muscular contraction, *J. Physiol. (London)*, 243, 1, 1974.
26. **Weiss, P. L., Kearney, R. E., and Hunter, I. W.,** Position dependence of ankle joint mechanics. II. Active mechanics, *J. Biomech.*, 19, 737, 1986.
27. **Agarwal, G. C., Goodarzi, S. M., O'Neill, W. D., and Gottlieb, G. L.,** Time series modeling of the neuromuscular system, *Biol. Cybern.*, 51, 103, 1984.
28. **Robles, S. S. and Soechting, J. F.,** Dynamic properties of the cat tenuissimus muscle, *Biol. Cybern.*, 33, 187, 1979.
29. **Hill, A. V.,** The heat of shortening and the dynamic constants of muscle, *Proc. R. Soc. London Ser. B*, 126, 136, 1938.

30. **Wilkie, D. R.**, The mechanical properties of muscle, *Br. Med. Bull.*, 12, 177, 1956.
31. **Ritchie, J. M. and Wilkie, D. R.**, The dynamics of muscular contraction, *J. Physiol. (Lond.)*, 143, 104, 1958.
32. **Hill, A.V.**, The abrupt transition from rest to activity in muscle, *Proc. R. Soc. London Ser. B*, 136, 399, 1949.
33. **Alexander, R. McN. and Vernon, A.**, The mechanics of hopping by kangaroos (macropodidae), *J. Zool. (London)*, 177, 265, 1975.
34. **Alexander, R. McN. and Bennet-Clark, H. C.**, Storage of elastic strain energy in muscle and other tissues, *Nature*, 265, 114, 1977.
35. **Ker, R. F., Dimery, N. J., and Alexander, R. McN.**, The role of tendon elasticity in hopping in a wallaby *(Macropus rufogriseus)*, *J. Zool. (London)*, 208, 417, 1986.
36. **Morgan, D. L., Proske, U., and Warren, D.**, Measurements of muscle stiffness and the mechanism of elastic storage of energy in hopping kangaroos, *J. Physiol. (London)*, 282, 253, 1978.
37. **Proske, U. and Morgan, D. L.**, Tendon stiffness: methods of measurement and significance for the control of movement. A review, *J. Biomech.*, 20, 75, 1987.
38. **Rack, P. M. H., Ross, H. F., Thilmann, A. F., and Walters, D. K. W.**, Reflex responses at the human ankle: the importance of tendon compliance, *J. Physiol. (London)*, 344, 503, 1983.
39. **Rack, P. M. and Westbury, D. R.**, Elastic properties of the cat soleus tendon and their functional importance, *J. Physiol. (London)*, 347, 479, 1984.
40. **McMahon, T. A.**, *Muscles, Reflexes, and Locomotion*, Princeton University Press, Princeton, NJ, 1984.
41. **Alexander, R. McN.**, Mechanics of skeleton and tendons, in *Handbook of Physiology. The Nervous System*, Section 1, Vol. 2 (Part 1), American Physiology Society, Bethesda, MD, 1981, chap. 2.
42. **Gans, C. and Bock, W. J.**, The functional significance of muscle architecture — a theoretical analysis, *Ergeb. Anat. Entwicklungsgesch.*, 38, 115, 1965.
43. **Gans, C.**, Fiber architecture and muscle function, *Exercise Sport Sci. Rev.*, 10, 160, 1982.
44. **Alexander, R. McN. and Vernon, A.**, The dimensions of knee and ankle muscles and the forces they exert, *J. Hum. Movement Stud.*, 1, 115, 1975.
45. **Otten, E.**, Concepts and models of functional architecture in skeletal muscle, *Exercise Sport Sci. Rev.*, in press.
46. **Gans, C. and de Vree, F.**, Functional bases of fiber length and angulation in muscle, *J. Morphol.*, 192, 63, 1987.
47. **Loeb, G. E., Pratt, C. A., Chanaud, C. M., and Richmond, F. J. R.**, Distribution and innervation of short, interdigitated muscle fibers in parallel-fibered muscles of the cat hindlimb, *J. Morphol.*, 191, 1, 1987.
48. **Richmond, F. J. R., MacGillis, D. R. R., and Scott, D. A.**, Muscle-fiber compartmentalization in cat splenius muscles, *J. Neurophysiol.*, 53, 868, 1985.
49. **Woledge, R. C., Curtin, N. A., and Homsher, E.**, *Energetic Aspects of Muscle Contraction*, Monographs of the Physiological Society No. 41, Academic Press, London, 1985.
50. **Morgan, D. L., Mochon, S., and Julian, F. J.**, A quantitative model of intersarcomere dynamics during fixed-end contractions of single frog muscle fibers, *Biophys. J.*, 39, 189, 1982.
51. **Lieber, R. L. and Baskin, R. J.**, Intersarcomere dynamics of single muscle fibers during fixed-end tetani, *J. Gen. Physiol.*, 82, 347, 1983.
52. **Morgan, D. L.**, From sarcomeres to whole muscles, *J. Exp. Biol.*, 115, 69, 1985.
53. **Burke, R. E.**, Motor units: anatomy, physiology, and functional organization, in *Handbook of Physiology. The Nervous System*, Sect. 1, Vol. 2 (Part 1), American Physiology Society, Bethesda, MD, 1981, chap. 10.
54. **Stein, R. B.**, Peripheral control of movement, *Physiol. Rev.*, 54, 215, 1974.
55. **De Luca, C. J.**, Control properties of motor units, *J. Exp. Biol.*, 115, 125, 1985.
56. **Burke, R. E., Levine, D. N., Tsairis, P., and Zajac, F. E., III**, Physiological type and histochemical profiles in motor units of the cat gastrocnemius, *J. Physiol. (London)*, 234, 723, 1973.
57. **Close, R. I.**, Dynamic properties of mammalian skeletal muscles, *Physiol. Rev.*, 52, 129, 1972.
58. **Bigland-Ritchie, B. and Woods, J. J.**, Changes in muscle contractile properties and neural control during human muscular fatigue, *Muscle Nerve*, 7, 691, 1984.
59. **De Luca, C. J.**, Myoelectrical manifestations of localized muscular fatigue in humans, *CRC Crit. Rev. Biomed. Eng.*, 11, 251, 1984.
60. **Edgerton, V. R., Roy, R. R., Gregor, R. J., and Rugg, S.**, Morphological basis of skeletal muscle power output, in *Human Muscle Power*, Jones, N. L., McCartney, N., and McComas, A. J., Eds., Human Kinetics Publishers, Inc., Illinois, 1986, chap. 4.

61. **Ramsey, R. W. and Street, S. F.**, The isometric length-tension diagram of isolated skeletal muscle fibers of the frog, *J. Cell. Comp. Physiol.*, 15, 11, 1940.
62. **Gordon, A. M., Huxley, A. F., and Julian, F. J.**, The variation in isometric tension with sarcomere length in vertebrate muscle fibres, *J. Physiol. (London)*, 184, 170, 1966.
63. **Edman, K. A. P.**, The relation between sarcomere length and active tension in isolated semitendinosus fibres of the frog, *J. Physiol. (London)*, 183, 407, 1966.
64. **Borg, T. K. and Caulfield, J. B.**, Morphology of connective tissue in skeletal muscle, *Tissue Cell*, 12, 197, 1980.
65. **Alnaqeeb, M. A., Al Zaid, N. S., and Goldspink, G.**, Connective tissue changes and physical properties of developing and ageing skeletal muscle, *J. Anat.*, 139, 667, 1984.
66. **Magid, A. and Law, D. J.**, Myofibrils bear most of the resting tension in frog skeletal muscle, *Science*, 230, 1280, 1985.
67. **Rack, P. M. H. and Westbury, D. R.**, The effects of lengths and stimulus rate on tension in the isometric cat soleus muscle, *J. Physiol. (London)*, 204, 443, 1969.
68. **Allen, J. D. and Moss, R. L.**, Factors influencing the ascending limb of the sarcomere length-tension relationship in rabbit skinned muscle fibres, *J. Physiol. (London)*, 390, 119, 1987.
69. **Abbott, B. C. and Wilkie, D. R.**, The relation between velocity of shortening and the tension-length curve of skeletal muscle, *J. Physiol. (London)*, 120, 214, 1953.
70. **Bahler, A. S., Fales, J. T., and Zierler, K. L.**, The dynamic properties of mammalian skeletal muscle, *J. Gen. Physiol.*, 51, 369, 1968.
71. **Matsumoto, Y.**, Validity of the force-velocity relation for muscle contraction in the length region, $l \leq l_0$, *J. Gen. Physiol.*, 50, 1125, 1967.
72. **Hatcher, D. D. and Luff, A. R.**, The effect of initial length on the shortening velocity of cat hind limb muscles, *Pflugers Arch.*, 407, 396, 1986.
73. **Edman, K. A. P.**, The velocity of unloaded shortening and its relation to sarcomere length and isometric force in vertebrate muscle fibres, *J. Physiol. (London)*, 291, 143, 1979.
74. **Julian, F. J.**, The effect of calcium on the force-velocity relation of briefly glycerinated frog muscle fibres, *J. Physiol. (London)*, 218, 117, 1971.
75. **Julian, F. J. and Moss, R. L.**, Effects of calcium and ionic strength on shortening velocity and tension development in frog skinned muscle fibres, *J. Physiol. (London)*, 311, 179, 1981.
76. **Moss, R. L.**, The effect of calcium on the maximum velocity of shortening in skinned skeletal muscle fibres of the rabbit, *J. Muscle Res. Cell Motil.*, 3, 295, 1982.
77. **Moss, R. L.**, Effects on shortening velocity of rabbit skeletal muscle due to variations in the level of thin-filament activation, *J. Physiol.*, 377, 497, 1986.
78. **Pierrynowski, M. R. and Morrison, J. B.**, A physiological model for the evaluation of muscular forces in human locomotion: theoretical aspects, *Math. Biosci.*, 75, 69, 1985.
79. **Hof, A. L. and Van den Berg, J. W.**, EMG to force processing I: an electrical analogue of the Hill muscle model, *J. Biomech.*, 14, 747, 1981.
80. **McCully, K. K. and Faulkner, J. A.**, Characteristics of lengthening contractions associated with injury to skeletal muscle fibers, *J. Appl. Physiol.*, 61, 293, 1986.
81. **Katz, B.**, The relation between force and speed in muscular contraction, *J. Physiol. (London)*, 96, 45, 1939.
82. **Joyce, G. C. and Rack, P. M. H.**, Isotonic lengthening and shortening movements of cat soleus muscle, *J. Physiol. (London)*, 204, 475, 1969.
83. **Mashima, H.**, Force-velocity relation and contractility in striated muscles, *Jpn. J. Physiol.*, 34, 1, 1984.
84. **Cavagna, G. A., Dusman, B., and Margaria, R.**, Positive work done by a previously stretched muscle, *J. Appl. Physiol.*, 24, 21, 1968.
85. **Cavagna, G. A. and Citterio, G.**, Effect of stretching on the elastic characteristics and the contractile component of frog striated muscle, *J. Physiol. (London)*, 239, 1, 1974.
86. **Edman, K. A. P., Elzinga, G., and Noble, M. I. M.**, Enhancement of mechanical performance by stretch during tetanic contractions of vertebrate skeletal muscle fibres, *J. Physiol. (London)*, 281, 139, 1978.
87. **Huxley, A. F. and Simmons, R. M.**, Proposed mechanism of force generation in striated muscle, *Nature*, 233, 533, 1971.
88. **Ford, L. E., Huxley, A. F., and Simmons, R. M.**, Tension responses to sudden length change in stimulated frog muscle fibers near slack length, *J. Physiol. (London)*, 269, 441, 1977.
89. **Julian, F. J. and Sollins, M. R.**, Variation of muscle stiffness with force at increasing speeds of shortening, *J. Gen. Physiol.*, 66, 287, 1975.
90. **Jewell, B. R. and Wilkie, D. R.**, An analysis of the mechanical components in frog's striated muscle, *J. Physiol. (London)*, 143, 515, 1958.

91. **Walmsley, B. and Proske, U.,** Comparison of stiffness of soleus and medial gastrocnemius muscles in cats, *J. Neurophysiol.*, 46, 250, 1981.
92. **Suzuki, S. and Sugi, H.,** Extensibility of the myofilaments in vertebrate skeletal muscle as revealed by stretching rigor muscle fibers, *J. Gen. Physiol.*, 81, 531, 1983.
93. **Cecchi, G., Griffiths, P. J., Lopez, J. R., Taylor, S., and Wanek, L. A.,** Calcium activation in skeletal muscle, in *Intracellular Calcium Regulation*, Bader, H., Gietzen, K., Rosenthal, J., Rudel, R., and Wolf, H. U., Eds., Manchester University Press, Manchester, England, 1986, 213.
94. **Ebashi S. and Endo, M.,** Calcium ion and muscle contractions, *Prog. Biophys. Mol. Biol.*, 18, 125, 1968.
95. **Taylor, C. P. S.,** Isometric muscle contraction and the active state: an analog computer study, *Biophys. J.*, 9, 759, 1969.
96. **Ma, S. and Zahalak, G. I.,** Simple calcium-activation dynamics for a distribution-moment model of muscle, *Proc. 9th Annu. Conf. IEEE Eng. Med. Biol. Soc.*, 1, 317, 1987.
97. **Ma, S. and Zahalak, G. I.,** Activation dynamics for a distribution-moment model of skeletal muscle, *Math. Comput. Modeling*, 11, 778, 1988.
98. **Moss, R. L.,** Sarcomere length-tension relations of frog skinned muscle fibres during calcium activation at short lengths, *J. Physiol. (London)*, 292, 177, 1979.
99. **Burke, R. E., Rudomin, P., and Zajac, F. E.,** A catch property in single mammalian motor units, *Science*, 168, 122, 1971.
100. **Burke, R. E., Rudomin, P., and Zajac, F. E.,** The effect of activation history on tension production by individual muscle units, *Brain Res.*, 109, 515, 1976.
101. **Zajac, F. E. and Young, J. L.,** Properties of stimulus trains producing maximum tension-time area per pulse from single motor units in medial gastrocnemius muscle of the cat, *J. Neurophysiol.*, 43, 1206, 1980.
102. **Stein, R. B. and Parmiggiani, F.,** Nonlinear summation of contractions in cat muscles. I. The early depression, *J. Gen. Physiol.*, 78, 227, 1981.
103. **Demieville, H. N. and Partridge, L. D.,** Probability of peripheral interaction between motor units and implications for motor control, *Am. J. Physiol.*, 238, R119, 1980.
104. **Winter, D. A.,** *Biomechanics of Human Movement*, John Wiley & Sons, New York, 1979.
105. **Hof, A.L., Prink, C. N. A., and van Best, J. A.,** Comparison between EMG to force processing and kinetic analysis for the calf muscle moment in walking and stepping, *J. Biomech.*, 20, 167, 1987.
106. **Gottlieb, G. L. and Agarwal, G. C.,** Filtering of electromyographic signals, *Am. J. Phys. Med.*, 49(2), 142, 1970.
106a. **Levine, W. S. and Zajac, F. E.,** unpublished analysis, 1984.
107. **Zheng, Y., Hemami, H., and Stokes, B. T.,** Muscle dynamics, size principle, and stability, *IEEE Trans. Biomed. Eng.*, BME-31, 489, 1984.
108. **De Luca, C. J. and Mambrito, B.,** Voluntary control of motor units in human antagonist muscles: coactivation and reciprocal activation, *J. Neurophysiol.*, 58, 525, 1987.
109. **Hoffer, J. A., Loeb, G. E., Marks, W. B., O'Donovan, M. J., Pratt, C. A., and Sugano, N.,** Cat hindlimb motoneurons during locomotion. I. Destination, axonal conduction velocity, and recruitment threshold, *J. Neurophysiol.*, 57, 510, 1987.
110. **Stephenson, D. G. and Williams, D. A.,** Effects of sarcomere length on the force-pCa relation in fast- and slow-twitch skinned muscle fibres from the rat, *J. Physiol. (London)*, 333, 637, 1982.
111. **Wells, J. B.,** Comparison of mechanical properties between slow and fast mammalian muscles, *J. Physiol. (London)*, 178, 252, 1965.
112. **Lannergren, J., Lindblom, P., and Johansson, B.,** Contractile properties of two varieties of twitch muscle fibres in *Xenopus laevis*, *Acta Physiol. Scand.*, 114, 523, 1982.
113. **Ranatunga, K. W.,** The force-velocity relation of rat fast- and slow-twitch muscles examined at different temperatures, *J. Physiol. (London)*, 351, 517, 1984.
114. **Faulkner, J. A., Claflin, D. R., and McCully, K. K.,** Power output of fast and slow fibers from human skeletal muscles, in *Human Muscle Power*, Jones, N. L., McCartney, N., and McComas, A. J., Eds., Human Kinetics Publishers, Illinois, 1986, chap. 6.
115. **Ariano, M. A., Armstrong, R. B., and Edgerton, V. R.,** Hindlimb muscle fiber populations of five mammals, *J. Histochem. Cytochem.*, 21, 51, 1973.
116. **Saltin, B. and Gollnick, P. D.,** Skeletal muscle adaptability: significance for metabolism and performance, in *Handbook of Physiology, The Nervous System*, Section 1, Vol. 2 (Part 1), American Physiology Society, Bethesda, MD, 1981, chap 19.
117. **Altringham, J. D. and Johnston, I. A.,** The pCa-tension and force-velocity characteristics of skinned fibres isolated from fish fast and slow muscles, *J. Physiol. (London)*, 333, 421, 1982.

118. **Spector, S. A., Gardiner, P. F., Zernicke, R. F., Roy, R. R., and Edgerton, V. R.,** Muscle architecture and force-velocity characteristics of cat soleus and medial gastrocnemius: implications for motor control. *J. Neurophysiol.*, 44, 951, 1980.
119. **Lännergren, J. and Westerblad, H.,** The temperature dependence of isometric contractions of single, intact fibres dissected from a mouse foot muscle, *J. Physiol.*, 390, 285, 1987.
120. **Ranatunga, K. W.,** Temperature-dependence of shortening velocity and rate of isometric tension development in rat skeletal muscle, *J. Physiol. (London)*, 329, 465, 1982.
121. **Sacks, R. D. and Roy, R. R.,** Architecture of the hind limb muscles of cats: functional significance, *J. Morphol.*, 173, 185, 1982.
122. **Wickiewicz, T. L., Roy, R. R., Powell, P. L., and Edgerton, V. R.,** Muscle architecture of the human lower limb, *Clin. Orthop.*, 179, 275, 1983.
123. **An, K. N., Hui, F. C., Morrey, B. F., Linscheid, R. L., and Chao, E. Y.,** Muscles across the elbow joint: a biomechanical analysis, *J. Biomech.*, 14, 659, 1981.
124. **Brand, P. W., Beach, R. B., and Thompson, D. E.,** Relative tension and potential excursion of muscles in the forearm and hand, *J. Hand Surg.*, 6, 209, 1980.
125. **Brand, R. A., Pedersen, D. R., and Friederich, J. A.,** The sensitivity of muscle force predictions to changes in physiologic cross-sectional area, *J. Biomech.*, 19, 589, 1986.
126. **Powell, P. L., Roy, R. R., Kanim, P., Bello, M. A., and Edgerton, V. R.,** Predictability of skeletal muscle tension from architectural determinations in guinea pig hindlimbs, *J. Appl. Physiol. Respirat. Environ. Exercise Physiol.*, 57, 1715, 1984.
127. **Stephenson, D. G. and Williams, D. A.,** Calcium-activated force response in fast- and slow-twitch skinned muscle fibres of the rat at different temperatures, *J. Physiol. (London)*, 317, 281, 1981.
128. **Claflin, D. R. and Faulkner, J. A.,** Shortening velocity extrapolated to zero load and unloaded shortening velocity of whole rat skeletal muscle, *J. Physiol.*, 359, 357, 1985.
129. **Bodine, S. C., Roy, R. R., Meadows, D. A., Zernicke, R. F., Sacks, R. D., Fournier, M., and Edgerton, V. R.,** Architectural, histochemical, and contractile characteristics of a unique biarticular muscle: the cat semitendinosus, *J. Neurophysiol.*, 48, 192, 1982.
130. **Fung, Y. C.,** *Biomechanics: Mechanical Properties of Living Tissue*, Springer-Verlag, New York, 1981.
131. **Butler, D. L., Grood, E. S., Noyes, F. R., and Zernicke, R. F.,** Biomechanics of ligaments and tendons, *Exercise Sport Sci. Rev.*, 6, 125, 1979.
132. **Butler, D. L., Grood, E. S., Noyes, F. R., Zernicke, R. F., and Brackett, K.,** Effects of structure and strain measurement technique on the material properties of young human tendons and fascia, *J. Biomech.*, 17, 579, 1984.
133. **Butler, D. L., Kay, M. D., and Stoffer, D. C.,** Comparison of material properties in fascicle-bone units from human patella tendon and knee ligaments, *J. Biomech.*, 19, 425, 1986.
134. **Herrick, W. C., Kingsbury, H. B., and Lou, D. Y. S.,** A study of the normal range of strain, strain rate, and stiffness of tendon, *J. Biomed. Mater. Res.*, 12, 877, 1978.
135. **Woo, S. L.-Y., Gomez, M. A., Amiel, D., Ritter, M. A., Gelberman, R. H., and Akeson, W. H.,** The effects of exercise on the biomechanical and biochemical properties of swine digital flexor tendons, *J. Biomech. Eng.*, 103, 51, 1981.
136. **Woo, S. L.-Y., Gomez, M. A., Woo, Y.-K., and Akeson, W. H.,** Mechanical properties of tendons and ligaments. II. The relationships of immobilization and exercise on tissue remodeling, *Biorheology*, 19, 397, 1982.
137. **Woo, S. L.-Y., Ritter, M. A., Amiel, D., Sanders, T. M., Gomez, M. A., Kuei, S. C., Garfin, S. R., and Akeson, W. H.,** The biomechanical and biochemical properties of swine tendons — long term effects of exercise on the digital extensors, *Connect. Tissue Res.*, 7, 177, 1980.
138. **Ker, R. F., Dimery, N. J., and Alexander, R. McN.,** The role of tendon elasticity in hopping in a wallaby (Macropus rufogriseus), *J. Zool. (London)*, 208, 417, 1986.
139. **Rack, P. M. H. and Ross, H. F.,** The tendon of flexor pollicis longus: its effects on the muscular control of force and position at the human thumb, *J. Physiol. (London)*, 351, 99, 1984.
140. **Alexander, R. McN., Maloiy, G. M. O., Ker, R. F., Jayes, A. S., and Warui, C. N.,** The role of tendon elasticity in the locomotion of the camel (Camelus dromedarius), *J. Zool. (London)*, 198, 293, 1982.
141. **Ker, R. F., Dimery, N. J., and Alexander, R. McN.,** The role of tendon elasticity in hopping in a wallaby *(Macropus rufogriseus)*, *J. Zool. (London)*, 208, 417, 1986.
142. **Bennett, M. B., Ker, R. F., Dimery, N. J., and Alexander, R. McN.,** Mechanical properties of various mammalian tendons, *J. Zool. (London)*, 209, 537, 1986.
143. **Woo, S. L.-Y.,** Mechanical properties of tendons and ligaments. I. Quasi-static and nonlinear viscoelastic properties, *Biorheology*, 19, 385, 1982.

144. **Hubbard, R. P. and Chun, K. J.**, Mechanical responses of tendons to repeated extension and wait periods, *J. Biomech. Eng.*, 110, 11, 1988.
145. **Ducati, A., Parmiggiani, F., and Schieppati, M.**, Simulation of post-tetanic potentiation and fatigue in muscle using a visco-elastic model, *Biol. Cybern.*, 44, 129, 1982.
146. **Oguztoreli, M. N. and Stein, R. B.**, Analysis of a model for antagonistic muscles, *Biol. Cybern.*, 45, 177, 1982.
147. **Oguztoreli, M. N. and Stein, R. B.**, Optimal control of antagonistic muscles, *Biol. Cybern.*, 48, 91, 1983.
148. **Wilkie, D. R.**, Measurement of the series elastic component at various times during a single muscle twitch, *J. Physiol. (London)*, 134, 527, 1956.
149. **Hill, A. V.**, The series elastic component of muscle, *Proc. R. Soc. London Ser. B*, 137, 273, 1950.
150. **Matsumoto, Y.**, Theoretical series elastic element length in Rana pipiens sartorius muscles, *J. Gen. Physiol.*, 50, 1139, 1967.
151. **Elliott, D. H. and Crawford, G. N. C.**, The thickness and collagen content of tendon relative to the strength and cross-sectional area of muscle, *Proc. R. Soc. London Ser. B*, 162, 137, 1965.
152. **Elliott, D. H.**, Structure and function of mammalian tendon, *Biol. Rev.*, 40, 392, 1965.
153. **Proske, U. and Morgan, D. L.**, Stiffness of cat soleus muscle and tendon during activation of part of muscle, *J. Neurophysiol.*, 52, 459, 1984.
154. **Ker, R. F.**, Elasticity of hand and forefoot tendons, unpublished manuscript.
155. **Dimery, N. J., Alexander, R. McN., and Ker, R. F.**, Elastic extension of leg tendons in the locomotion of horses *(Equus caballus)*, *J. Zool. (London)*, 210, 415, 1986.
156. **Zernicke, R. F., Garhammer, J., and Jobe, F. W.**, Human patellar-tendon rupture: a kinematic analysis, *J. Bone Jt. Surg.*, 59-A, 179, 1977.
157. **Komi, P. V.**, Biomechanics and neuromuscular performance, *Med. Sci. Sports Exercise*, 16, 26, 1984.
158. **Goslow, G. E., Jr., Reinking, R. M., and Stuart, D. G.**, The cat step cycle: hind limb joint angles and muscle lengths during unrestrained locomotion, *J. Morphol.*, 141, 1, 1973.
159. **Walmsley, B., Hodgson, J. A., and Burke, R. E.**, Forces produced by medial gastrocnemius and soleus muscles during locomotion in freely moving cats, *J. Neurophysiol.*, 41, 1203, 1978.
160. **Huijing, P. A.**, Architecture of the human gastrocnemius muscle and some functional consequences, *Acta Anat.*, 123, 101, 1985.
161. **Hoy, M. G., Zajac, F. E., and Gordon, M. E.**, A musculoskeletal model of the human lower extremity: the effect of muscle, tendon, and moment arm on the moment-angle relationship of musculotendon actuators at the hip, knee, and ankle, *J. Biomech.*, submitted.
161a. **Roy, R. R., DiGiuro, M. D., and Edgerton, V. R.**, Architectural design of adult cat hip musculature, *Soc. Neurosci. Abstr.*, 9, 359, 1983.
162. **Zajac, F. E., Topp, E. L., and Stevenson, P. J.**, A dimensionless musculotendon model, *Proc. 8th Ann. Conf. IEEE Eng. Med. Biol. Soc.*, Ft Worth, TX, 1986, 601.
163. **Hogan, N.**, The mechanics of multi-joint posture and movement control, *Biol. Cybern.*, 52, 315, 1985.
164. **Stein, R. B.**, What muscle variable(s) does the nervous system control in limb movements?, *Behav. Brain Sci.*, 5, 535, 1982.
165. **Zajac, F. E. and Faden, J. S.**, Relationship among recruitment order, axonal conduction velocity and muscle unit properties of type-identified motor units in cat plantaris muscle, *J. Neurophysiol.*, 53, 1303, 1985.
166. **Zajac, F. E.**, Coupling of recruitment order to the force produced by motor units: the "size principle hypothesis" revisited, in *The Segmental Motor System*, Binder, M. D. and Mendell, L. M., Eds., Oxford University Press, Oxford, in press.
167. **Antonsson, E. K. and Mann, R. W.**, The frequency content of gait, *J. Biomech.*, 18, 39, 1985.
168. **Winter, D. A.**, *The Biomechanics and Motor Control of Human Gait*, University of Waterloo Press, Waterloo, Canada, 1987.
169. **Bressler, B. H. and Clinch, N. F.**, The compliance of contracting skeletal muscle, *J. Physiol. (London)*, 237, 477, 1974.
170. **Rack, P. M. H., and Westbury, D. R.**, The short range stiffness of active mammalian muscle and its effect on mechanical properties, *J. Physiol. (London)*, 240, 331, 1974.
171. **Buller, A. J., Kean, C. J. C., Ranatunga, K. W., and Smith, J. M.**, Temperature dependence of isometric contractions of cat fast and slow skeletal muscles, *J. Physiol. (London)*, 355, 25, 1984.
172. **Bennett, A. F.**, Temperature and muscle, *J. Exp. Biol.*, 155, 333, 1985.
173. **Zahalak, G. I.**, A distribution-moment approximation for kinetic theories of muscular contraction, *Math. Biosci.*, 55, 89, 1981.